




ORIGINAL ARTICLE

WILEY

High time-resolution measurements of ultrafine and fine woodsmoke aerosol number and surface area concentrations in biomass burning kitchens: A case study in Western Kenya

Danielle N. Wagner^{1,2}  | Samuel R. Odhiambo³ | Rose M. Ayikukwei⁴  |
Brandon E. Boor^{1,2} 

¹Lyles School of Civil Engineering, Purdue University, West Lafayette, Indiana, USA

²Ray W. Herrick Laboratories, Center for High Performance Buildings, Purdue University, West Lafayette, Indiana, USA

³School of Engineering, Moi University, Eldoret, Kenya

⁴AMPATH Kenya, Eldoret, Kenya

Correspondence

Brandon E. Boor, Lyles School of Civil Engineering, Purdue University, West Lafayette, IN, USA.

Email: bboor@purdue.edu

Funding information

National Science Foundation, Grant/Award Number: CBET-1847493; Purdue University Shah Family Global Innovation Lab; American Society of Heating, Refrigerating, and Air Conditioning Engineers Graduate Student Grant-In-Aid Award

Abstract

Indoor air pollution associated with biomass combustion for cooking remains a significant environmental health challenge in rural regions of sub-Saharan Africa; however, routine monitoring of woodsmoke aerosol concentrations continues to remain sparse. There is a paucity of field data on concentrations of combustion-generated ultrafine particles, which efficiently deposit in the human respiratory system, in such environments. Field measurements of ultrafine and fine woodsmoke aerosol (diameter range: 10–2500 nm) with field-portable diffusion chargers were conducted across nine wood-burning kitchens in Nandi County, Kenya. High time-resolution measurements (1 Hz) revealed that indoor particle number (PN) and particle surface area (PSA) concentrations of ultrafine and fine woodsmoke aerosol are strongly temporally variant, reach exceedingly high levels ($PN > 10^6/\text{cm}^3$; $PSA > 10^4 \mu\text{m}^2/\text{cm}^3$) that are seldom observed in non-biomass burning environments, are influenced by kitchen architectural features, and are moderately to poorly correlated with carbon monoxide concentrations. In five kitchens, PN concentrations remained above $10^5/\text{cm}^3$ for more than half of the day due to frequent cooking episodes. Indoor/outdoor ratios of PN and PSA concentrations were greater than 10 in most kitchens and exceeded 100 in several kitchens. Notably, the use of metal chimneys significantly reduced indoor PN and PSA concentrations.

KEYWORDS

carbon monoxide, combustion, cookstove emissions, indoor air pollution, ultrafine particles, ventilation

1 | INTRODUCTION

1.1 | Scope and persistence of solid fuel combustion for cooking in indoor environments

In order to obtain global indoor air quality equity, it is imperative to target efforts in potential high-impact areas, which are often those limited in resources needed for improvement; yet the majority of

indoor air studies are focused on regions with a lower burden of disease.¹ Human exposure campaigns conducted in locations where people are the most vulnerable can compel risk studies linking indoor air pollution and individual health outcomes.¹ Modeling data that is collected in real situations can be used to predict wider exposure trends and potential public health advancements that can result from achieving worldwide indoor air quality improvements.² Such exposure research combined with evidence of successful

This is an open access article under the terms of the [Creative Commons Attribution-NonCommercial](https://creativecommons.org/licenses/by-nc/4.0/) License, which permits use, distribution and reproduction in any medium, provided the original work is properly cited and is not used for commercial purposes.

© 2022 The Authors. *Indoor Air* published by John Wiley & Sons Ltd.

intervention strategies can then help inform regional policy changes to impact local change.¹

With over 4 million attributed annual deaths, exposure to indoor air pollution from the combustion of solid fuels is the eighth highest risk factor of global mortality.^{3,4} Due to a lack of access to electricity, about 2.5 billion people depend on solid fuels for their daily cooking needs,⁵ including over 90% of rural regions of sub-Saharan Africa and several countries in Asia⁶; this dependence is expected to rise in areas where population growth will outpace technology advancement.⁷ Exposure-response investigations note causal inference between woodsmoke aerosol concentrations and the development of health issues, including acute respiratory lung infection, chronic obstructive pulmonary disease, and lung cancer.⁸ Exposure to woodsmoke aerosol can decrease quality of life by triggering asthma attacks, contributing to unhealthy pregnancies, and causing cataracts, which may require surgeries to prevent blindness.¹

Because of these well-established health effects, ongoing research to improve indoor air quality explores biomass combustion emission-reducing techniques or decreases the residence time of woodsmoke aerosol indoors. A major facet of this research includes investigating more efficient combustion techniques, or cookstoves improved relative to three stone fires (TSFs).^{9–13} In addition to reducing fugitive stove emissions indoors, increasing natural ventilation by modifying kitchen architectural features is a mitigation method that can reduce the amount of time woodsmoke aerosol is highly concentrated indoors. Some campaigns focus on kitchen parameters (materials, orientation, openings),¹⁴ while others combine indoor emission reduction with ventilation by enclosing biomass stoves, such as with clay or bricks, which allows a routed combustion chamber as well as a dedicated woodsmoke outlet that may be fitted with a chimney or vented directly outside.^{15,16} Some campaigns evaluate the effects of modifying specific architectural or ventilation features, as well as source emissions.^{10,17–19}

Metrics used to report baseline stove emissions and gauge the efficacy of stove and architectural modifications for environmental health and climate implications commonly include (but are not limited to) mass-based particle measurements,^{9–11,15,20} black carbon,^{11,12} and/or elemental carbon⁹; and are often represented in a variety of ways: either as directly measured concentrations,²¹ modified combustion efficiencies,^{22,23} particle size characterizations,²⁴ composition,¹⁸ emission rates,⁹ or emission factors.⁹ Measurements may be made in multiple locations, including, but not limited to, those chosen to reflect personal monitoring,²⁵ the breathing zone,^{11,12,17,21} or bulk air.²⁵

1.2 | Indoor woodsmoke aerosol concentration metrics and health linkages

Indoor concentrations of woodsmoke aerosol can be measured in units of particle number (PN, /cm³), particle surface area (PSA, μm²/cm³), lung deposited surface area (LDSA, μm²/cm³), particle volume (PV, μm³/cm³), and particle mass (PM, μg/m³). The suitability of each

Practical Implications

Combustion-generated nano-sized ultrafine particles (diameter ≤ 100 nm) are associated with adverse human health outcomes due to their ability to penetrate to the deepest regions of the lung. This study provides new field data on temporal variations in particle number and surface area concentrations of combustion-generated ultrafine particles in biomass burning indoor environments in Western Kenya, where such data are severely lacking. Diffusion chargers were found to enable multi-day, non-intrusive monitoring of nano-sized ultrafine particles among rural communities in sub-Saharan Africa that are disproportionately impacted by indoor air pollution. Such field measurements can benefit future modeling and exposure assessment studies.

concentration metric depends in part on the size range of the particles of interest. Generally, ultrafine particles (UFP; $D_p \leq 100$ nm) and fine particles (FP; $100 \text{ nm} < D_p \leq 2500$ nm) are *together* best represented by PN, PSA, and LDSA concentrations given the significant contribution of ultrafine and fine particles (UFP + FP) toward PN and PSA size distributions.^{26–30} Fine and coarse particles (CP; $D_p > 2500$ nm) are *together* best represented by PV and PM concentrations as they dominate PV and PM size distributions.^{28,31,32} The PM concentration for $D_p \leq 2500$ nm, referred to as PM_{2.5}, is a widely used metric in cookstove research. However, other metrics, such as PN and PSA, can better account for sub-100 nm particles produced by biofuel combustion and can provide valuable information regarding exposure to ultrafine woodsmoke aerosol.

The physiochemical properties of woodsmoke aerosol vary during different combustion stages. Smoldering and intermediate combustion can be characterized as generating fewer, larger ash particles, primarily in the FP size fraction.^{33,34} Inhalation of these particles has been linked to dose-dependent cytotoxic inflammation,³⁵ and further DNA damage is associated with higher levels of surface-adsorbed organics, such as polycyclic aromatic hydrocarbons and quinones.^{33,34} Because of these health outcomes, measurement of PSA concentrations is strongly recommended for examining toxicity.³⁶ Efficient and flaming combustion stages have been shown to release high PN concentrations of UFPs.^{33,34} Cleaner flames tend to generate more refined, sub-100 nm soot aggregates.^{37,38} Inhaled combustion-generated UFPs coated in organics and transition metals can cause systemic inflammation via combined oxidative and bio-transformative effects with different types of epithelial cells.^{33,34,39–41} Combustion-generated UFPs can reduce the diversity of the gut microbiome when ingested (via mucociliary clearance) and induce neurotoxicity when coated with gas-phase organics resulting from incomplete combustion.^{42–45}

Indoor biomass combustion during use of traditional and improved stoves has been shown to result in PN size distributions that

are dominated by sub-300nm particles (Figure 1). Modal diameters of stove-emitted PN size distributions range from $D_p \sim 15$ nm for an air injection stove to $D_p \sim 150$ nm for a *chulha* stove. Importantly, there is significant overlap between stove-emitted PN size distributions and size-resolved total and regional deposition fractions for the human respiratory tract. The maximum of the deposition fraction curves for the pulmonary region ($D_p \sim 20$ nm) and tracheobronchial region ($D_p \sim 4$ nm) occurs in the UFP regime, while deposition in the head airways increases with decreasing particle size for $D_p < 300$ nm. Thus, woodsmoke aerosol measurements should consider concentration metrics (e.g. PN, PSA) that can better represent sub-300nm UFP+FPs that can efficiently deposit in the respiratory tract. Because mass-based metrics capture larger particles ($D_p > 100$ nm) and overlook the contribution of the more numerous UFPs that tend to dominate PN size distributions, traditional proxies for indoor air pollution (e.g. $PM_{2.5}$) can misrepresent health linkages.^{46–50} Recent air quality guidelines from the World Health Organization hint at, but do not reflect, the rising evidence of UFP toxicity in inhalation exposure standards.^{50,51} Field studies reporting PN and PSA concentrations of UFP+FPs in biomass burning indoor environments will contribute to developing new risk assessments and standards that can guide cookstove interventions.

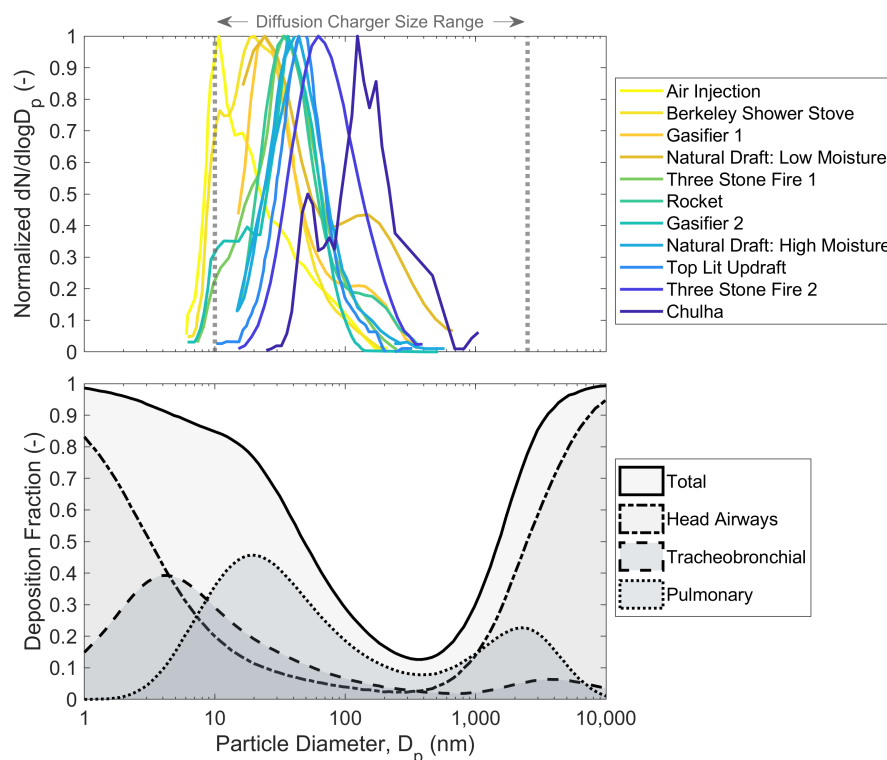
1.3 | Field measurements of indoor ultrafine and fine woodsmoke aerosol with diffusion chargers

There is a paucity of field data on PN and PSA concentrations of UFP+FPs during combustion of solid fuels for cooking in indoor environments in rural regions of sub-Saharan Africa, Asia, and

Central America. Real-time measurements of UFP+FPs that capture temporal variations in woodsmoke aerosol emissions and exposures are especially lacking. This is due in part to the challenges inherent in field deployment of laboratory-grade aerosol instrumentation that can detect sub-300nm particles, such as condensation particle counters (CPCs) and scanning mobility particle sizers (SMPSs). Notably, sub-300nm particles escape detection by most optical-based aerosol instruments that are widely used in cookstove studies.^{52–54} The limited existing data suggest indoor PN concentrations of UFP+FPs can reach upwards of $10^6/\text{cm}^3$.^{24,46,55,56} High time-resolution monitoring of UFP+FPs in households that use solid fuels requires instrumentation that can operate in conditions with little to no electricity in a non-intrusive manner to residents, can withstand high PN and PSA concentrations, and fit in smaller spaces.

Electrical particle charging-based aerosol instrumentation, such as diffusion chargers, has emerged as a suitable technique for real-time characterization of indoor UFP+FPs in biomass burning environments. Diffusion chargers utilize a unipolar charger (e.g. corona needle) to charge particles which are then detected via a sensitive electrometer. The current measured by the electrometer is translated to PN, PSA, LDSA, or PM concentrations through various techniques. Diffusion chargers have been used for measuring UFP+FPs in various field and laboratory settings, as discussed in the Supporting Information section. Most diffusion chargers are battery-powered and can measure high PN and PSA concentrations without the need for dilution of sample air. Diffusion chargers can charge and detect particles from $D_p \sim 10$ to 2500 nm,^{57–60} thereby capturing the majority of woodsmoke aerosol on a number-basis (Figure 1).

FIGURE 1 (top) Normalized stove-emitted particle number size distributions ($dN/d\log D_p$) and (bottom) size-resolved regional and total particle deposition fractions for the human respiratory tract. Particle number size distributions were taken from measurements of emissions of biomass combustion from a variety of stove designs: air injection¹¹², Berkeley shower⁴⁷, gasifier 1⁴⁹ and 2¹¹⁷, natural draft: low moisture and high moisture⁸⁸, three stone fire 1⁴⁷ and 2⁴⁹, rocket⁴⁹, top lit updraft¹⁰⁷, and *chulha*.¹¹⁸ Regional and total particle deposition fractions were taken from a semi-empirical model based on an adult during nasal breathing while sitting.¹¹⁹ The measurement size range ($D_p \sim 10$ –2500 nm) of the diffusion charger used in the field measurements in the kitchens in Nandi County, Kenya, is noted.



1.4 | Study objective

The objective of this study is to conduct real-time (1 Hz) measurements of PN and PSA concentrations of ultrafine and fine woodsmoke aerosol in biomass burning kitchens in Western Kenya through use of field-portable diffusion chargers. Indoor/outdoor (I/O) ratios of PN and PSA concentrations are evaluated, along with relationships between PN and PSA concentrations with carbon monoxide (CO) concentrations. To the authors' knowledge, this represents the first field investigation into indoor UFP+FPs generated from wood-burning stoves in East Africa. Such measurements expand knowledge regarding in situ exposures to sub-300 nm woodsmoke aerosol in households that utilize solid fuel combustion in a region of the world that experiences a high burden of disease due to indoor air pollution.

2 | MATERIALS AND METHODS

2.1 | Site description: biomass burning kitchens in Nandi County, Kenya

The field measurement campaign was conducted across nine kitchens located in Nandi County, Kenya. Out of an approximate population of 890 000 residents in Nandi County,⁶¹ an estimated 89% of households use firewood for cooking and 0.22% use electricity.⁶² Kitchens were selected through coordination with AMPATH Kenya^{63–65} based on willingness-to-participate and accessibility from main roads. The nine kitchens (K1 to K9) represent a range of styles incorporating different vernacular approaches to wood-burning stove design and building ventilation, as summarized in Table 1. The field campaign spanned the dry (January) and wet (June to July) seasons and included 47 days of sampling.

The Nandi kitchens include some that had been built in the past 10 years and some that had been recently modified with additional ventilation pathways, such as stove chimneys, extra façade openings in the form of windows or gaps between the tops of walls and the roof, and roof ridge vents allowing for buoyancy-driven airflow to the outdoors. Eight kitchens utilized enclosed clay stoves containing a warming compartment (*chepkuba*), as is common in Nandi County, and one used a TSF. Nandi homes are built with the kitchen as a stand-alone structure, separate from the main living area. Meals often start with morning tea and breakfast, sometimes an afternoon lunch, usually an afternoon tea, and then supper for children and then adults along with evening warming of food. Each Nandi-designed stove includes 2 or 3 burners, built with three soil types,⁶⁶ with bricks for structural support.

2.2 | Measurement of indoor ultrafine and fine woodsmoke aerosol and carbon monoxide

Size-integrated PN and PSA concentrations of ultrafine and fine woodsmoke aerosol were measured in real-time (1 Hz) with four

battery-powered diffusion chargers (Pegasor AQ Indoor, Pegasor Oy). The diffusion chargers have an operational range of $D_p \sim 10\text{--}2500\text{ nm}$ (Figure 1); the latter is established with a cyclone pre-separator and can measure PN concentrations from $<10^1$ to $>10^7/\text{cm}^3$.^{60,67} Their design is similar to the Pegasor Particle Sensor-M (PPS-M, Pegasor Oy), which is used for monitoring UFP+FPs in vehicle exhaust.^{57,68–70} The internal operation of the diffusion charger contributes to its field robustness: after a protected corona needle ionizes a steady stream of filtered air, the sample particles are then mixed with this air.⁶⁷ The charged particles are then detected by an electrometer in real-time, where the measured electrical current is directly related to the size-integrated PSA concentration, and the PN concentration is simultaneously reported based on manufacturer-calibrated algorithms.⁶⁷ The diffusion chargers were housed in custom-built enclosures at a central location within the kitchen, approximately 0.5 m from the stove. A copper tube was used to extract air 1.5 m above the floor. The diffusion chargers were serviced in the morning and sampled continuously across their battery life of 10–12 h; this span accounted for nearly all cooking-related activities. CO was measured with four battery-powered electrochemical sensors (EL-USB-CO300, Lascar Electronics Ltd.). The CO sensors have a time resolution of 15 s and an upper concentration limit of 300 ppm, which was exceeded on several occasions. Each day, the diffusion chargers and CO sensors sampled outdoor air in locations away from ventilated woodsmoke for about 30 min to calculate I/O ratios for PN, PSA, and CO concentrations. Zero checks for the diffusion chargers were taken daily by attaching a HEPA filter capsule to the inlet to ensure PN concentrations remained $<10^1/\text{cm}^3$.

2.3 | Calibration of diffusion chargers and co-location measurements

The four diffusion chargers used during the field campaign were calibrated against a water-based CPC (wCPC, Model 3788, TSI Inc.) using electrical mobility-classified NaCl and KCl particles (25, 50, 100, 200, and 300 nm) produced by a thermal aerosol generator.⁷¹ The electrical mobility diameter range of the NaCl and KCl particles represents typical modal diameters of woodsmoke aerosol produced by biomass burning stoves (Figure 1). PN and PSA concentrations of the NaCl and KCl particles spanned from 10^1 to $10^6/\text{cm}^3$ and 10^0 to $10^5 \mu\text{m}^2/\text{cm}^3$, respectively (Figure S1); this is representative of the range in PN and PSA concentrations measured during the field campaign. The results of linear regressions of aggregated PN and PSA concentrations measured by the four diffusion chargers with the wCPC are shown in Figure S1. Each slope (m) is used as a calibration coefficient for the respective instrument to correct the raw PN and PSA concentrations reported by the diffusion chargers ($m = 0.58$ for PN and $m = 1.17$ for PSA). Pearson's correlation coefficients (r) were determined to estimate the dependence of the diffusion charger values on the wCPC values ($r = 0.97$ for PN and $r = 0.91$ for PSA), using *corrcoef* in MATLAB (The MathWorks Inc.) with a 95% confidence interval.

TABLE 1 Summary of kitchen architectural features.

Kitchen ID	Ventilation type	Volume (m ³)	Stove type	No. of stove burners	Stove chimney	Roof ridge vent	Roof-wall gap	No. of windows
K1	Enhanced	22.7	Chepkube	3	Yes	Yes	Yes	1
K2	Enhanced	14.9	Chepkube	3	Yes	No	Yes	1
K3	Conventional	13.6	Chepkube	3	No	No	Yes	1
K4	Conventional	16.6	Chepkube	3	No	No	Yes	1
K5	Conventional	16.9	Three stone fire	1 (open)	No	No	No	1
K6	Conventional	22.8	Chepkube	3	No	No	Yes	1
K7	Conventional	12.5	Chepkube	3	No	No	No	1
K8	Conventional	27.7	Chepkube	3	No	No	No	1
K9	Enhanced	24.3	Chepkube	2	Yes	Yes	Yes	2

Note: K8 contained a thatch roof, all other kitchens featured an aluminum roof.

Both laboratory and field co-location measurements of the four diffusion chargers and four CO sensors were routinely completed during the field campaign (Figure S2). The laboratory and field co-location measurements were aggregated to determine correlation coefficients and *r*-values for each instrument based on a linear regression of each instrument's individual response vs. the mean response reported by all four instruments (Table S1). The correlation coefficients were used to adjust the PN (corrected after wCPC calibration), PSA (corrected after wCPC calibration), and CO (raw, derived from manufacturer calibration) concentrations reported by each instrument to account for instrument-to-instrument variability.

3 | RESULTS AND DISCUSSION

3.1 | Temporal variations in PN and PSA concentrations of ultrafine and fine woodsmoke aerosol

Real-time measurements with field-portable diffusion chargers revealed unique time-dependent variations in indoor PN and PSA concentrations of ultrafine and fine woodsmoke aerosol across nine biomass burning kitchens in Nandi County, Kenya. Characteristic diurnal profiles of indoor PN and PSA concentrations of UFP+FPs in each of the separate Nandi kitchens are illustrated in Figure 2, and CO concentration diurnal profiles are shown in Figure S7. Diurnal profiles varied in shape and magnitude among the kitchens due to variations in source and loss processes of combustion-generated UFP+FPs. The former is dependent on kitchen-specific cooking activities, stove design, and stove combustion conditions; the latter is primarily driven by differences in kitchen design that affect indoor-to-outdoor transport of woodsmoke aerosol due to buoyancy- and wind-driven natural ventilation. In general, stove emissions drove sudden increases in PN and PSA concentrations that were then sustained for extended periods before initiation of gradual decays toward background levels. Temporal profiles in PSA concentrations tended to follow those of PN concentrations (Figures 2–4). Figures 2

and 3 and Figure S7 were created by combining all relevant PN, PSA, or CO concentration measurements from the selected kitchens into 3-min intervals throughout an entire day, followed by taking the median or mean (as shown).

Among the nine Nandi kitchens, indoor PN concentrations spanned from 10^3 to $>10^6/\text{cm}^3$ and indoor PSA concentrations spanned from 10^2 to $10^5 \mu\text{m}^2/\text{cm}^3$ (Figures S3 and S4). The highest median PN and PSA concentrations were observed in K6, with $\text{PN} = 1.1 \times 10^6/\text{cm}^3$ and $\text{PSA} = 3 \times 10^4 \mu\text{m}^2/\text{cm}^3$, followed by K8 with $\text{PN} = 3.7 \times 10^5/\text{cm}^3$ and $\text{PSA} = 1.3 \times 10^4 \mu\text{m}^2/\text{cm}^3$; K7 with $\text{PN} = 2.9 \times 10^5/\text{cm}^3$ and $\text{PSA} = 9.9 \times 10^3 \mu\text{m}^2/\text{cm}^3$; K4 with $\text{PN} = 2.6 \times 10^5/\text{cm}^3$ and $\text{PSA} = 5.5 \times 10^3 \mu\text{m}^2/\text{cm}^3$; K5 with $\text{PN} = 1.4 \times 10^5/\text{cm}^3$ and $\text{PSA} = 4.6 \times 10^3 \mu\text{m}^2/\text{cm}^3$; K1 with $\text{PN} = 7.7 \times 10^4/\text{cm}^3$ and $\text{PSA} = 2.1 \times 10^3 \mu\text{m}^2/\text{cm}^3$; K2 with $\text{PN} = 1.9 \times 10^4/\text{cm}^3$ and $\text{PSA} = 1.9 \times 10^2 \mu\text{m}^2/\text{cm}^3$; K3 with $\text{PN} = 1.0 \times 10^4/\text{cm}^3$ and $\text{PSA} = 1.8 \times 10^2 \mu\text{m}^2/\text{cm}^3$; and K9 with $\text{PN} = 7.7 \times 10^3/\text{cm}^3$ and $\text{PSA} = 2.9 \times 10^2 \mu\text{m}^2/\text{cm}^3$. Each kitchen exhibited wide variability in PN and PSA concentrations across the entire field campaign, with inter-quartile ranges for each varying by one to two orders of magnitude (Figure S4). This variability persisted after sorting the concentrations among six periods designated as observed times of common combustion events (Figure 4). PN and PSA concentrations were least variable from 19:00 to 21:00, likely due to routine evening meal preparation times. Human health implications of the observed PN and PSA concentrations are difficult to discern given the lack of exposure standards based on such metrics. However, the Social and Economic Council of the Netherlands recommends an 8 h mean PN concentration limit for UFPs of $4 \times 10^4/\text{cm}^3$, which was commonly exceeded in the Nandi kitchens.^{72,73} Only K9 had a mean PN ($4.25 \times 10^4/\text{cm}^3$) close to this limit.

The diffusion charger measurements demonstrate that indoor PN and PSA concentrations remain elevated for a substantial fraction of the day in most kitchens due to frequent and repeated cooking episodes associated with morning, afternoon, and evening meal preparation (Figures 2 and 4). Similar trends can be seen in the CO concentration time series (Figure S7). Sustained periods with PN concentrations $>10^5/\text{cm}^3$ were observed in K4–K8, with intermittent

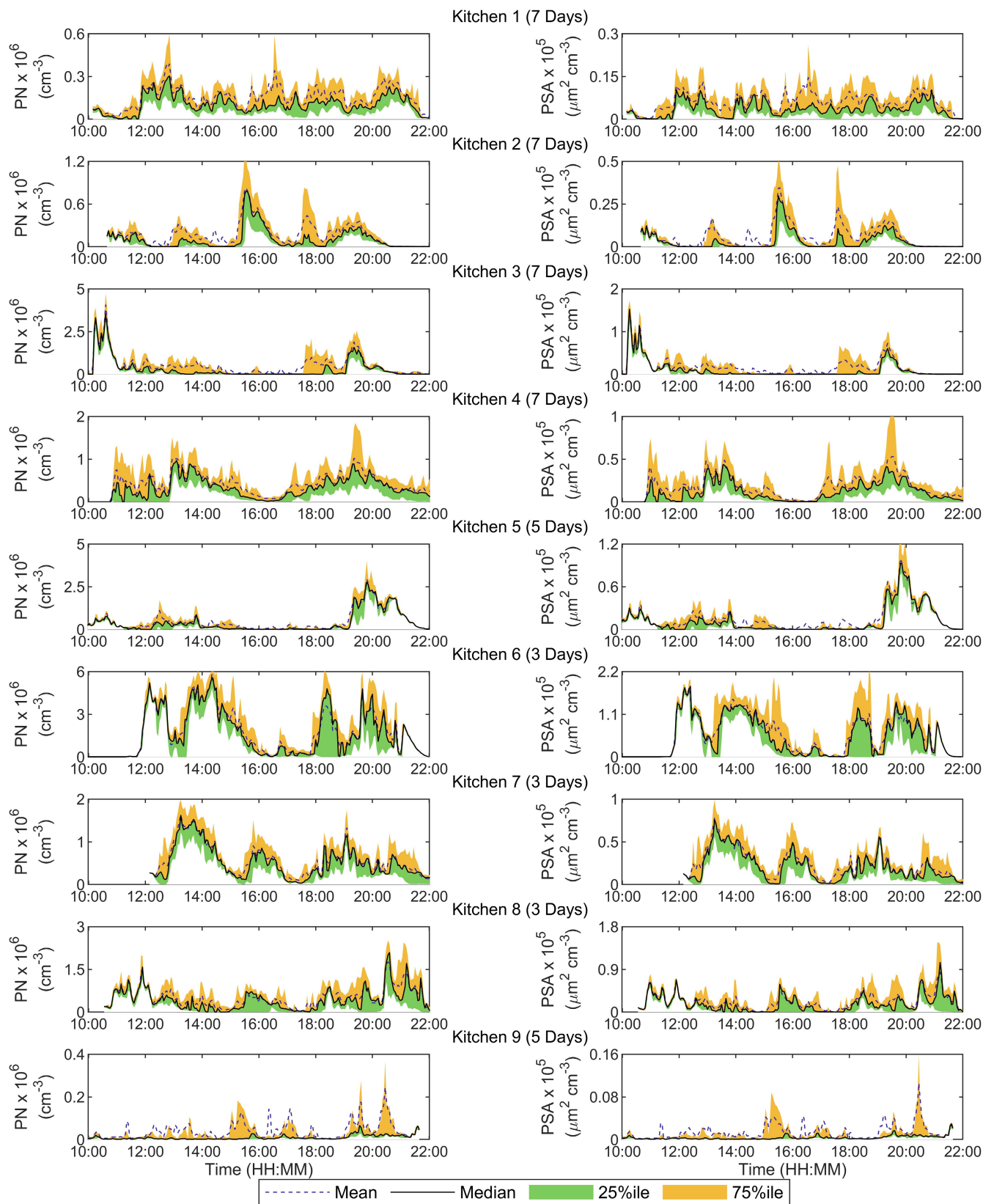
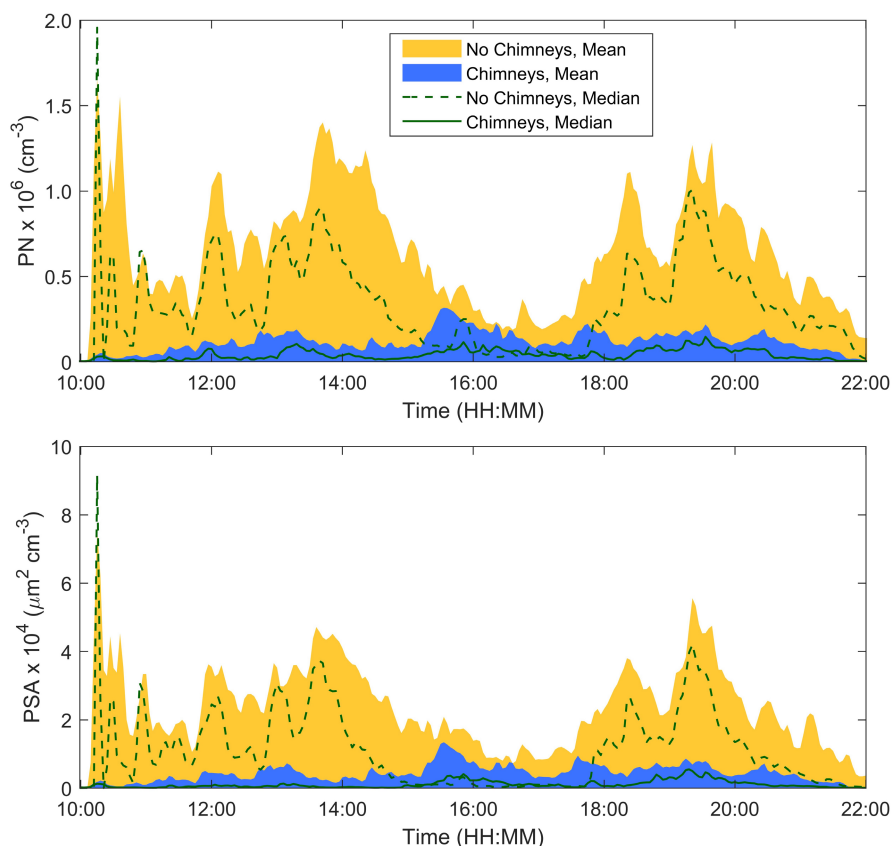


FIGURE 2 Characteristic diurnal profiles of indoor PN (left) and PSA (right) concentrations measured in each kitchen in Nandi County, Kenya. The dashed blue lines indicate the mean, the solid black lines indicate the median, and the green and orange lines indicate the 25th and 75th percentiles, respectively. Note that each y-axis is scaled differently to improve visualization of temporal variations in PN and PSA concentrations in each kitchen.

FIGURE 3 Characteristic diurnal profiles of indoor PN (top) and PSA (bottom) concentrations among kitchens with *chepkuba* stoves that either include a chimney (blue: K1, K2, K9) or do not include a chimney (orange: K3, K4, K6, K7, K8). Data are combined for each category in 3-min segments over the course of a day. The solid colors (blue, orange) indicate the mean and the dashed and solid green lines indicate the median.



peak PN concentrations often $>10^6/\text{cm}^3$. Table 2 lists the percentage of time PN concentrations exceeded three thresholds: $10^4/\text{cm}^3$, $5 \times 10^4/\text{cm}^3$, and $10^5/\text{cm}^3$. Six of the kitchens (K1, K4–K8) experienced PN concentrations exceeding $10^4/\text{cm}^3$, typical of levels measured in urban outdoor areas,^{74,75} for more than 75% of the day. Furthermore, PN concentrations above $10^5/\text{cm}^3$, comparable or greater than levels measured in traffic-impacted outdoor areas near roadways,^{53,76,77} were measured for more than half the day in five kitchens (K4–K8). Field measurements of UFP+FPs in non-biomass burning residential indoor environments rarely reveal such temporal trends as sources tend to be more episodic and elevated PN concentrations are seldom sustained for multi-hour periods.^{29,78–81} Interestingly, the diurnal profiles of UFP+FPs for the Nandi kitchens (K2, K6, K7) are qualitatively similar to that observed during the HOMEChem Thanksgiving Day event, during which cooking occurred for much of the day.²⁷

Some kitchens exhibited routine peak PN and PSA concentrations at about the same time each day, suggesting that some of the families have regular daily cooking times (Figures 2 and 4). For example, K2 has discernible peaks at approximately 11:30, 13:00, 15:30, 18:00, and 19:00, and K7 has peaks at around 13:30 and 16:00, followed by high concentration events dispersed throughout the evening. K6 has four prominent peaks at around 12:00, 14:00, 18:00, and 20:00, with noticeable oscillations in PN and PSA concentrations around each peak. Among all kitchens, K3 had the most distinct morning meal peak at around 10:00. Other kitchens exhibit less prominent peaks in their diurnal profiles, such as K1, K8, and

K9, likely due to greater variability in the timing and intensity of cooking-related emission events. Periods during which the highest PN and PSA concentrations were routinely observed varied among the kitchens, likely due to differences in stove use profiles. Elevated concentrations after 21:00 may be due to the periodic use of the wood-burning stoves for indoor space heating.^{5,82}

The wide range in the magnitude of the characteristic diurnal PN and PSA profiles is due in part to differences in the architectural features of the Nandi kitchens (Table 1). To better visualize the impact of adding intentional ventilation features to the kitchens, Figure 3 exhibits diurnal trends in PN and PSA concentrations among *chepkuba* kitchens with a chimney (K1, K2, K9: aggregated together) and without a chimney (K3, K4, K6, K7, K8: aggregated together). Three of the four lowest PN and PSA concentrations of UFP+FPs were measured in *chepkuba* kitchens with a chimney (K1, K2, K9). K9 had the flattest PN and PSA diurnal profiles of all kitchens; only a few minor peaks were detected and PN concentrations seldom exceeded $10^5/\text{cm}^3$. Along with a chimney, K9 incorporated a roof ridge vent, a roof-wall gap, and two windows – the most of all kitchens. Notably, the two windows were located on the NW and SE walls which facilitated wind-driven cross-ventilation due to the predominant wind direction in Nandi County (from NW). The higher 90th percentile PN and PSA concentrations in K2 as compared to K1 (Figure S4) may be due to the periodic use of a removable diffusion plate installed in the K2 chimney to reduce the amount of heat drawn from the stove.

It is evident that the additional natural ventilation pathways aided in reducing indoor levels of ultrafine and fine woodsmoke

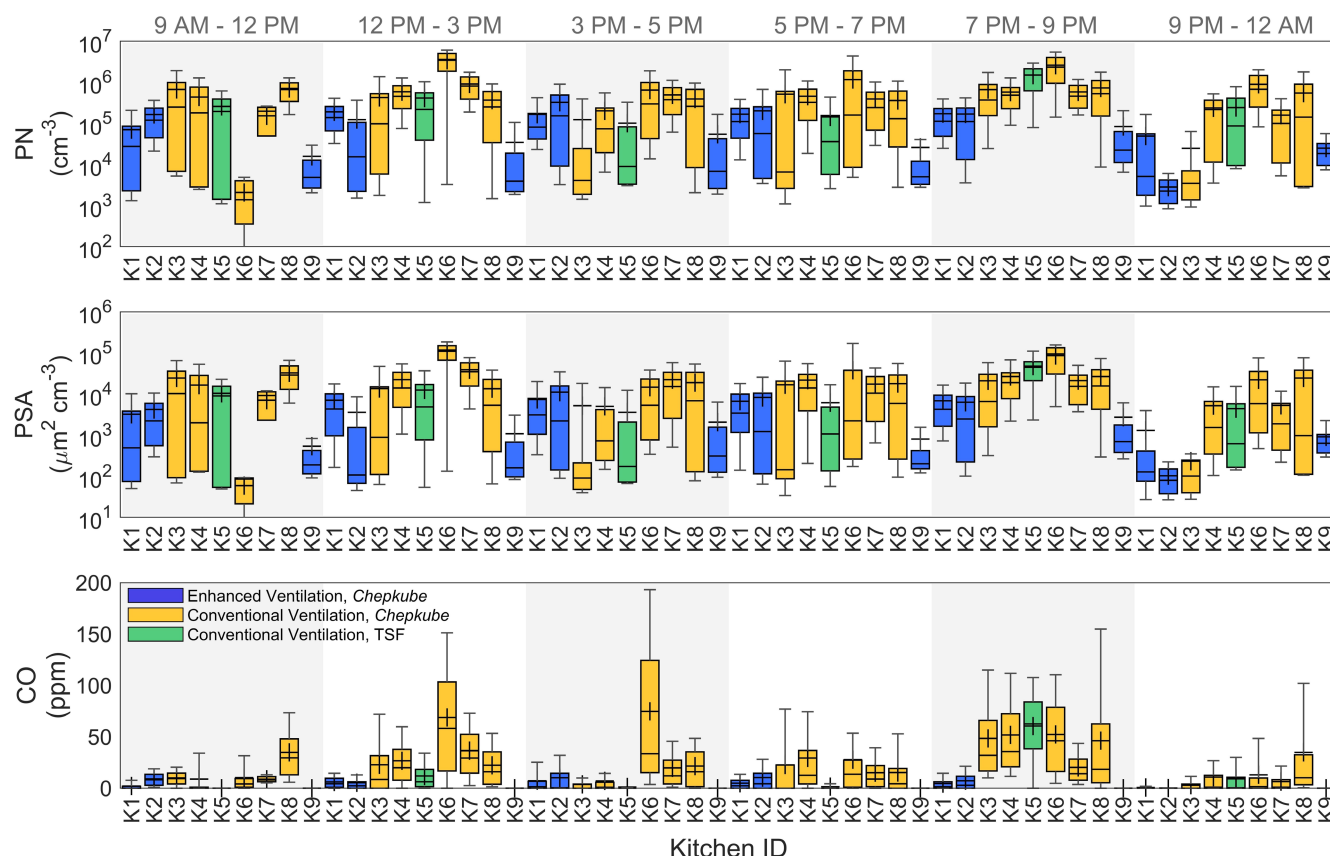


FIGURE 4 Indoor PN (top), PSA (middle), and CO (bottom) concentrations measured in each kitchen in Nandi County, Kenya.

Concentrations are sorted into six time periods: 9 AM to 12 PM, 12 PM to 3 PM, 3 PM to 5 PM, 5 PM to 7 PM, 7 PM to 9 PM, and 9 PM to 12 AM. Box plots represent the interquartile range, the middle horizontal lines represent the median, whiskers represent the 10th and 90th percentiles, and “+” markers represent the mean. Boxplot colors denote whether a kitchen was built for enhanced ventilation with a *chepkuba* stove (blue: K1, K2, K9), conventional ventilation with a *chepkuba* stove (orange: K3, K4, K6, K7, K8), or conventional ventilation with a three stone fire (TSF) (green: K5).

TABLE 2 Percentage of time that indoor PN concentrations exceeded different PN thresholds.

	Kitchen ID	K1	K2	K3	K4	K5	K6	K7	K8	K9
% of time exceeding PN threshold	10 000/cm ³	78	53	50	82	85	87	90	90	43
	50 000/cm ³	60	42	41	72	65	79	76	83	16
	100 000/cm ³	43	34	38	67	55	75	71	76	10

aerosol as compared to more traditional Nandi kitchen designs. PN and PSA concentrations in K5, which utilized a TSF, were similar to those using *chepkubes* without chimneys (K4, K7); however, the evening peak was greater than that observed in K4 and K7. K6, which had the highest PN and PSA concentrations throughout much of the day, was oriented in such a way that wind was observed to blow parallel to the window and door, reducing the likelihood of wind-driven cross-ventilation. For K7, the lack of a roof-wall gap and small volume (12.5 m³) compared to other kitchens with similar *chepkubes* likely contributed to the high PN and PSA concentrations that were observed (third highest of all kitchens). A Wilcoxon rank sum test performed using rank sum in MATLAB comparing a larger kitchen (K8: volume = 27.7 m³) and a smaller kitchen (K7: volume = 12.5 m³) resulted in a rejection of the null hypothesis of equivalence, implying

that the medians are significantly different (PN and PSA for K8 > K7). It is notable that K8 also contains a thatch roof; thus, even though K7 and K8 have the same number of burners and windows, the difference in PN and PSA concentrations may be due to comparing a larger thatch roof kitchen to a smaller aluminum roof kitchen. Comparing K1 (volume = 22.7 m³) and K2 (volume = 14.9 m³) also resulted in conclusion of non-equivalence, however, with the larger kitchen having lower concentrations. Thus, there cannot be any clear conclusions drawn about volume size and UFP+FP concentrations in these kitchens without a much larger random sampling of the various architectural styles, likely because it is difficult to control for other factors. Using the same test, a comparison between *chepkuba* kitchens with chimneys and enhanced ventilation pathways (K1, K2, K9) compared to those with no chimneys and conventional ventilation

(K3, K4, K6, K7, K8) also resulted in a significant difference between the two.

3.2 | Comparisons with PN and PSA concentrations of ultrafine and fine particles in biomass and non-biomass burning indoor environments

Field measurements of PN and PSA concentrations of UFP+FPs in biomass burning environments in rural regions of sub-Saharan Africa, Asia, and Central America are limited. However, extant data suggest similar trends as observed in the Nandi kitchens. Emissions from TSFs and rocket stoves in kitchens in Senegal were highly transient during cooking, with mean PN concentrations of 2.6 and $1.7 \times 10^6/\text{cm}^3$, respectively, closely resembling levels in K6.¹⁹ Cooking with open-fire and *justa* stoves in kitchens in Honduras was associated with 24h mean PN concentrations of $1.3 \times 10^5/\text{cm}^3$ and $9.1 \times 10^4/\text{cm}^3$, respectively, similar to several Nandi kitchens, while enclosed *justa* stoves consistently yielded lower emissions.⁸³ A study in Bangladesh reported mean PN concentrations of $7.5 \pm 3.1 \times 10^4/\text{cm}^3$ during cooking in kitchens using BCSIR improved stoves, similar to levels in K1, K2, and K5.⁸⁴ A metal chimney stove used for heating a living room in Bhutan resulted in PN concentrations that varied between $2 \times 10^5/\text{cm}^3$ and $2.5 \times 10^6/\text{cm}^3$.⁵⁶ Coal- and wood-burning stoves in Guizhou, China yielded PN concentrations from $5 \times 10^6/\text{cm}^3$ to $3 \times 10^7/\text{cm}^3$, greater than levels in K6.²⁴ Notably, the Nandi-based *chepkuba* with chimneys (K1, K2, K9), *justa* (Honduras), and BCSIR (Bangladesh) are all clay stoves that direct woodsmoke toward an attached chimney.^{83,84} This construction allows people to continue to operate their stoves in traditional ways, using the same biofuels, while decreasing PN concentrations. Few studies have reported PSA or LDSA concentrations. U-shaped clay cookstoves in Udaipur, India, produced LDSA concentrations of $5 \times 10^4 \mu\text{m}^2/\text{cm}^3$ (while LDSA \neq PSA, LDSA value is on the same order of magnitude as PSA in K6),⁴⁶ while kerosene stoves produced PSA concentrations of $1.1 \times 10^3 \mu\text{m}^2/\text{cm}^3$ (similar to K1).⁵⁵ It is important to note that the diurnal profiles presented here highlight the intensity of UFP+FP emissions throughout the day. In a laboratory study comparing particle emission rates of a TSF to several improved cookstoves, the TSF generated particles in the $D_p = 5\text{--}100\text{nm}$ size fraction at a magnitude around $10^{12}/\text{s}$; $D_p = 100\text{--}1000\text{nm}$ at $10^{11}/\text{s}$; and $D_p = 1000\text{--}2500\text{nm}$ at $<10^8/\text{s}$.⁴⁷ Because the larger size fractions would account for most of the mass, using total mass concentrations would likely not capture the intense number-based emission peaks of the sub-100nm UFPs.

Comparatively more field measurements of PN and PSA concentrations of UFP+FPs have been made during cooking in non-biomass burning indoor environments, primarily mechanically and naturally ventilated residences using gas and electric stoves. Collectively, results suggest that gas stoves are associated with PN concentrations ranging from 10^4 to $10^6/\text{cm}^3$, depending on cooking and kitchen ventilation conditions,^{27,81,85,86} while electric resistance and induction

stoves tend to produce lower PN concentrations ($10^3\text{--}10^5/\text{cm}^3$).²⁹ The range in indoor PN concentrations for gas and electric stoves span those observed among the Nandi kitchens using *chepkubes* with and without chimneys; however, the physiochemical properties of the particles are expected to vary widely among the stove types.^{87,88}

An important distinction between cooking in biomass and non-biomass burning environments is the duration of the UFP+FP emission events. Cooking events associated with gas and electric stoves in residences in North America, Europe, and Asia tend to be short ($<1\text{ h}$) and infrequent.^{27,81,86,89–91} This is in contrast to the Nandi kitchens, where multi-hour periods with elevated PN concentrations ($>10^5/\text{cm}^3$) are routinely observed (Table 2, Figure 2). Similar trends have been documented in other kitchens using open solid fuel combustion, demonstrating that stoves are actively used for multi-hour periods, resulting in persistent emission peaks.^{19,83,92} The total number or surface area of inhaled UFP+FPs depends not only on the magnitude of the PN or PSA concentration, respectively, but the duration of exposure. Extended periods of elevated levels of ultrafine and fine woodsmoke aerosol in Nandi kitchens and other biomass burning kitchens demonstrate the significant exposure potential of such indoor environments. Despite this, real-time indoor exposure data on sub-300nm UFP+FPs continue to remain sparse.

3.3 | Indoor/outdoor (I/O) ratios of PN and PSA concentrations

Indoor/outdoor ratios of PN and PSA concentrations were determined for each of the nine Nandi kitchens. In general, the indoor abundance of UFP+FPs was substantially higher than in adjacent outdoor areas. Outdoor PN and PSA concentrations are summarized in Figure 5, Figures S3 and S5; median concentrations across all kitchens and all days were $4 \times 10^3/\text{cm}^3$ and $1.2 \times 10^2 \mu\text{m}^2/\text{cm}^3$, respectively. The outdoor PN concentrations are similar to those observed in rural and clean background sites in locations around the world.⁹³ Outdoor CO concentrations were often close or equal to 0, thus, I/O ratios for CO were not estimated. On a few occasions, outdoor PN and CO concentrations exceeded $2 \times 10^4/\text{cm}^3$ and 10 ppm, respectively, possibly due to entrainment of ventilated woodsmoke at the outdoor sampling location. Unmaintained engine exhaust and trash burning likely contributed to the observed levels of UFP+FPs in Nandi County.^{93,94} There are few measurements of outdoor PN and PSA concentrations in rural regions of Africa, with most studies focused on upper atmospheric measurements of biomass burning emissions^{95–98} and Saharan desert dust aerosol.⁹⁹ Median outdoor PN concentrations of 1.04 and $5.14 \times 10^4/\text{cm}^3$ were measured in Accra, Ghana and Cairo, Egypt, respectively, greater than typical levels in Nandi.¹⁰⁰

As PN and PSA concentrations in the Nandi kitchens were much greater than outdoor levels, I/O ratios of UFP+FPs were often in the range of 10^0 to 10^2 (Figure 5). K6 and K7 were associated with the highest I/O ratios, with mean PN values of 9.2 and 2.9×10^2 and mean

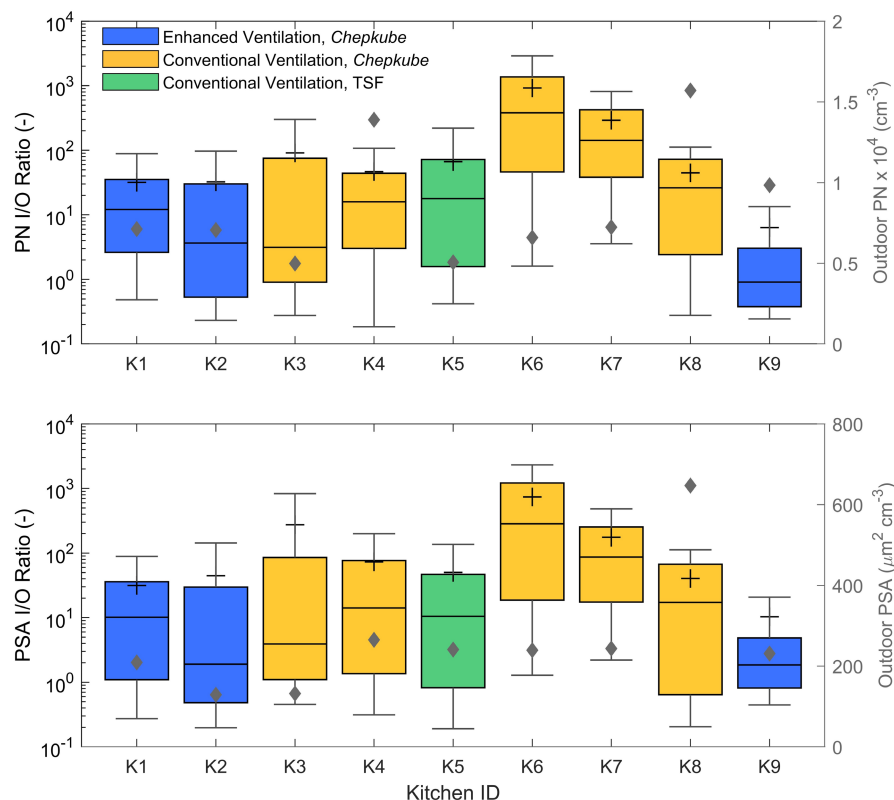


FIGURE 5 (left axis) Indoor/outdoor (I/O) ratios for PN (top) and PSA (bottom) concentrations and (right axis) median outdoor PN (top) and PSA (bottom) concentrations ("diamond" markers) for each kitchen in Nandi County, Kenya. The I/O ratio box plots represent the interquartile range, the middle horizontal lines represent the median, whiskers represent the 10th and 90th percentiles, and "+" markers represent the mean. Boxplot colors denote whether a kitchen was built for enhanced ventilation with a *chepkuba* stove (blue: K1, K2, K9), conventional ventilation with a *chepkuba* stove (orange: K3, K4, K6, K7, K8), or conventional ventilation with a three stone fire (TSF) (green: K5). Note the different y-axis scales for the I/O ratios (log) and outdoor concentrations (linear).

PSA values of 7.4 and 1.8×10^2 , respectively (Table S2). Indoor PN concentrations periodically exceeded $10^6/\text{cm}^3$ in K6, resulting in I/O ratios breaching 10^3 . The lowest I/O ratios were observed in K9, with mean PN and PSA values of 6.4 and 10 , respectively. I/O ratios below unity were occasionally observed in K1-K5, K8, and K9 during periods when PN and PSA concentrations decayed to background levels following combustion events. Notably, the I/O ratios for PN concentrations of UFP + FPs in the Nandi kitchens far exceed those reported for urban residences in North America, Europe, and Asia, which typically span from 0.1 to 2 .^{29,86,101,102} The low I/O ratios reported in these studies are due in part to high outdoor PN concentrations in urban air, less frequent activation of cooking and non-cooking UFP + FP sources, and indoor particle removal via active filtration systems. I/O ratios of UFP + FPs provide a useful basis to compare the relative magnitude of indoor and outdoor air pollution at a particular site, as well as the relative importance of indoor and outdoor sources of aerosol exposure. It is evident that use of wood-burning stoves in Nandi kitchens creates atmospheres that starkly contrast their proximate outdoor spaces. Such high I/O ratios suggest real-time indoor monitoring of sub- 300nm UFP + FPs with diffusion chargers should be made a greater priority than outdoor monitoring in Nandi County and similar regions in rural sub-Saharan Africa.

3.4 | Patterns of correlations between indoor PN and PSA concentrations with CO concentrations

In contrast to PN and PSA concentrations of ultrafine and fine woodsmoke aerosol, CO concentrations are commonly

measured during field campaigns in biomass burning environments.^{46,56,84,103-105} Studies have evaluated $\text{PM}_{2.5}$ -CO concentration correlations in kitchens using wood-burning stoves,^{46,84,103,105-107} however, little is known regarding PN-CO and PSA-CO relationships in such environments nor if CO can be used to predict levels of UFP + FPs. Figure 6 presents kitchen-resolved paired PN and CO concentration measurements, paired PSA and CO concentration measurements, and associated Pearson correlation coefficients (as r -values) for each (Table 3). PN and PSA concentrations were time-averaged based on the time resolution of the CO sensors (15 s). Additional comparisons are made showing PN-CO and PSA-CO relationships (Table S3, Figure S6) among kitchens with enhanced ventilation with a *chepkuba* stove (K1, K2, K9) and kitchens with conventional ventilation with a *chepkuba* stove (K3, K4, K6, K7, K8). Among these data, there is no notable difference in correlation strength between enhanced and conventionally ventilated kitchens (Figure 6 and Figure S6).

The results presented in Figure 6 demonstrate that there is wide variability in the relationship between PN and PSA concentrations of UFP + FPs with CO concentrations in the Nandi kitchens. The kitchens exhibit a range of positive r -values for the paired stationary PN-CO and PSA-CO measurements (r -value range: 0.20 – 0.74). The strongest correlations were identified in K5 (PN-CO r -value: 0.72 , PSA-CO r -value: 0.74) and K8 (PN-CO r -value: 0.68 , PSA-CO r -value: 0.65), and the weakest correlations were identified in K9 (PN-CO r -value: 0.20 , PSA-CO r -value: 0.21) and K6 (PN-CO r -value: 0.36 , PSA-CO r -value: 0.30). For each kitchen, the r -values for the PN-CO and PSA-CO relationships are close,

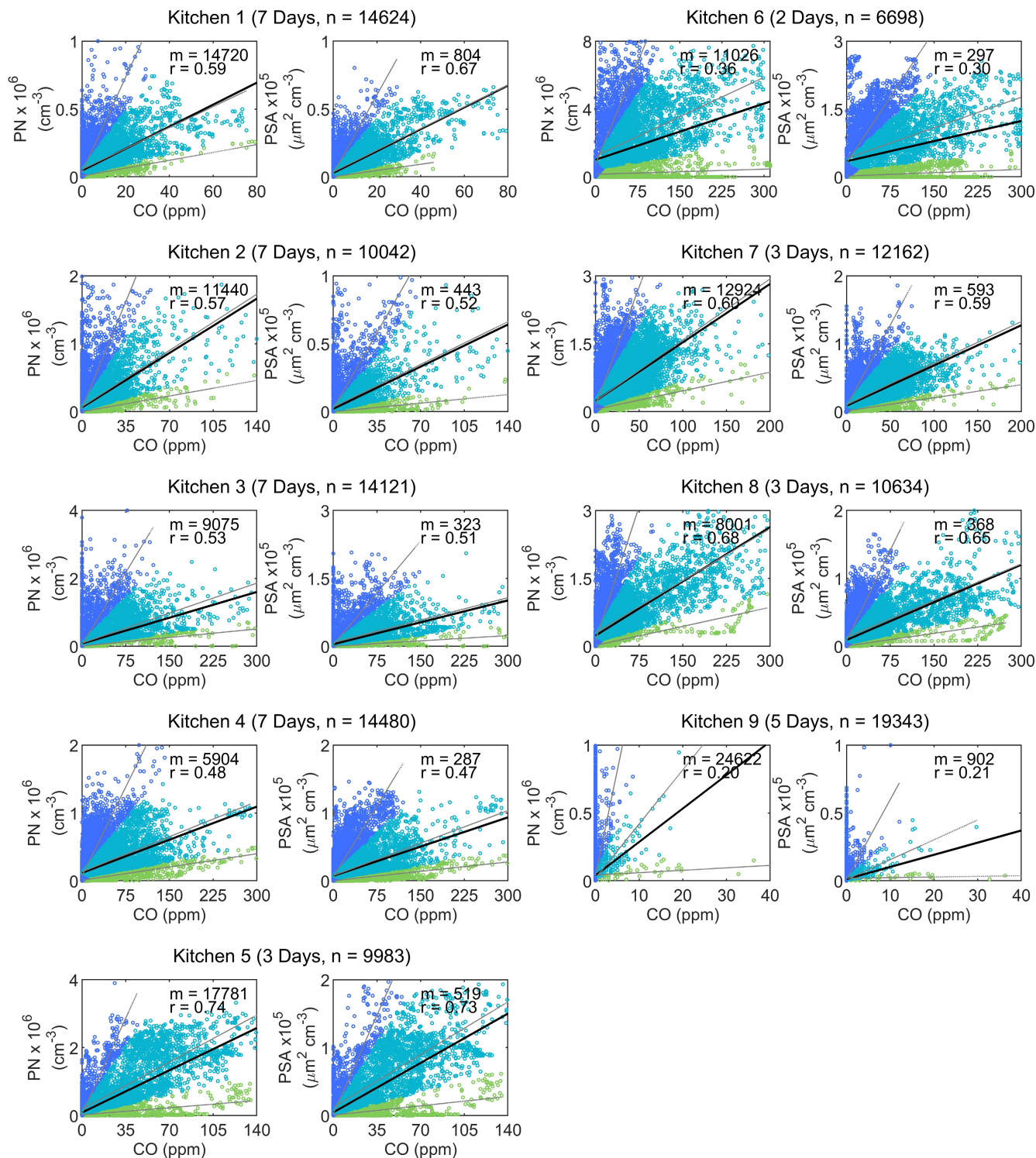


FIGURE 6 Paired indoor PN and CO concentration measurements and paired indoor PSA and CO concentration measurements in each kitchen in Nandi County, Kenya. The Pearson correlation coefficient (r), slope (m), and number of samples (n) for each PN-CO and PSA-CO relationship are shown. The overall linear fit (solid black line) was determined without forcing the y-intercept to zero. Each PN-CO and PSA-CO concentration pair is categorized by one of the following three regimes (Table 3): (1) high UFP + FPs, low CO (near y-axis; blue markers), (2) symmetric UFP + FPs and CO (near linear regression line; teal markers), and (3) high CO, low UFP + FPs (near x-axis; green markers). The linear fits for each of the three regimes are also shown (dashed gray lines).

TABLE 3 Summary of indoor PN-CO and PSA-CO correlation analysis (Figure 6) and percentage of PN-CO and PSA-CO concentration pairs in each regime. For each kitchen, the regime with the highest *r*-value is denoted in bold font (for PN and PSA).

<i>r</i> -value for all UFP + FP and CO data		Percentage of PN-CO and PSA-CO concentration pairs in each regime					
PN-CO	PSA-CO	Kitchen ID	Regime 1: high UFP + FPs, low CO (near y-axis)		Regime 2: symmetric UFP + FPs and CO (near linear regression line)		Regime 3: high CO, low UFP + FPs (near x-axis)
0.59	0.67	K1	PN: 61%, <i>r</i> -value: 0.77, <i>m</i> : 6.4×10^4	PSA: 59% <i>r</i> -value: 0.78, <i>m</i> : 2.9×10^3	PN: 30%, <i>r</i> -value: 0.77, <i>m</i> : 1.4×10^4	PSA: 27%, <i>r</i> -value: 0.83, <i>m</i> : 800	PN: 9%, <i>r</i> -value: 0.90, <i>m</i> : 5.3×10^3 PSA: 14%, <i>r</i> -value: 0.81, <i>m</i> : 230
0.57	0.52	K2	PN: 55%, <i>r</i> -value: 0.77, <i>m</i> : 4.5×10^4	PSA: 46%, <i>r</i> -value: 0.76, <i>m</i> : 1.6×10^3	PN: 26%, <i>r</i> -value: 0.80, <i>m</i> : 1.2×10^4	PSA: 27%, <i>r</i> -value: 0.79, <i>m</i> : 450	PN: 19%, <i>r</i> -value: 0.87, <i>m</i> : 3.3×10^3 PSA: 27%, <i>r</i> -value: 0.74, <i>m</i> : 90
0.53	0.51	K3	PN: 50%, <i>r</i> -value: 0.79, <i>m</i> : 5.1×10^4	PSA: 52%, <i>r</i> -value: 0.80, <i>m</i> : 1.5×10^3	PN: 30%, <i>r</i> -value: 0.73, <i>m</i> : 1.1×10^4	PSA: 20%, <i>r</i> -value: 0.83, <i>m</i> : 330	PN: 20%, <i>r</i> -value: 0.83, <i>m</i> : 3.0×10^3 PSA: 28%, <i>r</i> -value: 0.76, <i>m</i> : 79
0.48	0.47	K4	PN: 46%, <i>r</i> -value: 0.82, <i>m</i> : 3.2×10^4	PSA: 43%, <i>r</i> -value: 0.85, <i>m</i> : 1.4×10^3	PN: 33%, <i>r</i> -value: 0.69, <i>m</i> : 6.3×10^3	PSA: 26%, <i>r</i> -value: 0.76, <i>m</i> : 320	PN: 21%, <i>r</i> -value: 0.88, <i>m</i> : 2.4×10^3 PSA: 31%, <i>r</i> -value: 0.83, <i>m</i> : 93
0.72	0.74	K5	PN: 58%, <i>r</i> -value: 0.90, <i>m</i> : 8.1×10^4	PSA: 57%, <i>r</i> -value: 0.90, <i>m</i> : 2.1×10^3	PN: 29%, <i>r</i> -value: 0.80, <i>m</i> : 2.0×10^4	PSA: 25%, <i>r</i> -value: 0.79, <i>m</i> : 550	PN: 13%, <i>r</i> -value: 0.64, <i>m</i> : 3.0×10^3 PSA: 18%, <i>r</i> -value: 0.67, <i>m</i> : 98
0.36	0.30	K6	PN: 27%, <i>r</i> -value: 0.82, <i>m</i> : 8.0×10^4	PSA: 34%, <i>r</i> -value: 0.78, <i>m</i> : 1.9×10^3	PN: 38%, <i>r</i> -value: 0.61, <i>m</i> : 1.5×10^4	PSA: 27%, <i>r</i> -value: 0.66, <i>m</i> : 450	PN: 35%, <i>r</i> -value: 0.25, <i>m</i> : 1.0×10^3 PSA: 39%, <i>r</i> -value: 0.38, <i>m</i> : 49
0.60	0.59	K7	PN: 36%, <i>r</i> -value: 0.81, <i>m</i> : 5.2×10^4	PSA: 30%, <i>r</i> -value: 0.81, <i>m</i> : 2.4×10^3	PN: 48%, <i>r</i> -value: 0.76, <i>m</i> : 1.4×10^4	PSA: 43%, <i>r</i> -value: 0.74, <i>m</i> : 610	PN: 16%, <i>r</i> -value: 0.85, <i>m</i> : 4.1×10^3 PSA: 27%, <i>r</i> -value: 0.85, <i>m</i> : 190
0.68	0.65	K8	PN: 34%, <i>r</i> -value: 0.80, <i>m</i> : 3.9×10^4	PSA: 29%, <i>r</i> -value: 0.84, <i>m</i> : 1.8×10^3	PN: 42%, <i>r</i> -value: 0.83, <i>m</i> : 7.7×10^3	PSA: 36%, <i>r</i> -value: 0.80, <i>m</i> : 360	PN: 24%, <i>r</i> -value: 0.88, <i>m</i> : 2.8×10^3 PSA: 37%, <i>r</i> -value: 0.88, <i>m</i> : 120
0.20	0.21	K9	PN: 99%, <i>r</i> -value: 0.35, <i>m</i> : 1.5×10^5	PSA: 99%, <i>r</i> -value: 0.37, <i>m</i> : 5.9×10^3	PN: 0.8%, <i>r</i> -value: 0.84, <i>m</i> : 4.0×10^4	PSA: 0.8%, <i>r</i> -value: 0.84, <i>m</i> : 1.5×10^3	PN: 0.2%, <i>r</i> -value: 0.52, <i>m</i> : 1.8×10^3 PSA: 0.2%, <i>r</i> -value: 0.35, <i>m</i> : 47

and there is no discernable trend of CO relating more closely to PN or PSA. The strength of the PN-CO and PSA-CO correlations was not related to the presence of a stove chimney or additional ventilation pathways; however, the strongest correlation for both was found in the kitchen using a TSF (K5).

The PN-CO and PSA-CO correlation plots were partitioned into three regimes to evaluate time-dependent changes in the relative production of UFP+FPs and CO by the wood-burning stoves (Figure 6, Table 3). Using triangulation, the distance of each datapoint was determined to be more proximal to either the lines $x = 0$ (regime 1, blue markers), $x = y$ (regime 2, teal markers), or $y = 0$ (regime 3, green markers). Because the magnitude of the difference between the CO and PN or PSA concentrations is so large, the concentrations were normalized by the maximum CO, PN, or PSA concentration before determining the estimated difference of each datapoint from each line. Regime 1 represents periods when greater quantities of UFP+FPs are emitted relative to CO, such that associated PN-CO and PSA-CO pairs cluster along the y-axis, where $PN \gg CO$ and $PSA \gg CO$. Regime 2 represents periods when comparatively similar amounts of UFP+FPs and CO are emitted, such that associated PN-CO and PSA-CO pairs cluster around the linear regression line, where $PN \sim CO$ and $PSA \sim CO$. Regime 3 represents periods when comparatively greater quantities of CO are emitted relative to UFP+FPs, such that associated PN-CO and PSA-CO pairs cluster along the x-axis, where $CO \gg PN$ and $CO \gg PSA$. Table 3 lists the percentage of measured PN-CO and PSA-CO pairs in each of the three regimes for each kitchen. The patterns that arise within and between kitchens when viewing the PN-CO and PSA-CO relationships as three regimes highlight the importance of measuring both analytes (UFP+FPs, CO), as one could easily be lower while the other is higher, depending on the stove operational conditions.

Periods when the wood-burning stoves produced high PN or PSA concentrations and relatively low CO concentrations were common in many of the Nandi kitchens. More than 50% of the paired PN-CO measurements were located in regime 1 for five kitchens: K1, K2, K3, K5, and K9; data in K9 almost exclusively fell into this regime with CO often close to zero (Figures 4 and 6, Figure S7). In most kitchens, PN concentrations exceeded $5 \times 10^5/\text{cm}^3$ during periods with sub-25 ppm levels of CO. When considering the aggregate PN-CO and PSA-CO data presented in Figure 6, it is evident that CO is a poor proxy for UFP+FPs during regime 1 periods. Increased number-based emissions of UFP+FPs along with lower emissions of CO may indicate more efficient and flaming combustion within the Nandi stoves due to sufficient oxygen supply and higher combustion temperatures.⁸⁷

By viewing the correlation values within each regime (Table 3), it can be seen that regime 1 or 3 generally had the strongest correlations among the three regimes, except for the kitchens with enhanced ventilation (K1, K2, K9). Regime 3 was the least frequently observed regime in most kitchens. Regime 3 may indicate smoldering combustion within the wood-burning stoves. Combustion conditions characterized by low temperatures with less air mixing and less available solid fuel surface area tend to generate larger, more

spherical organic carbon particles with $D_p > 100\text{nm}$, lower number concentrations of UFP+FPs, and greater amounts of CO.^{87,108} The percentage of PSA-CO pairs in regime 3 was greater than that for PN-CO pairs for all nine kitchens; this may suggest a greater abundance of particles larger than $D_p \sim 100\text{nm}$ which tend to contribute strongly to PSA size distributions.

The low-to-moderate PN-CO and PSA-CO correlations suggest that CO concentrations are not a valid surrogate for PN or PSA concentrations of UFP+FPs in biomass burning environments. Similar results have been documented for $PM_{2.5}$ -CO relationships. Carter et al¹⁰⁶ compiled $PM_{2.5}$ -CO correlations from field measurements of biomass combustion during cooking across different countries and fuel types. The r -value across all studies was low (r -value: 0.36) and varied between 0.22 and 0.68 for studies conducted in Tanzania, Peru, The Gambia, China, India, and Honduras. Similar results were reported by Patel et al¹⁰⁷ for PSA-CO correlations (r -value: 0.65) of improved cookstove emissions. This range in r -values is consistent with the PN-CO and PSA-CO correlations seen in the Nandi kitchens. The extent of scatter observed in the correlation comparisons may be due in part to the heterogenous nature of biomass, which can cause multiple combustion stages to occur at the same time in different areas of the fire, thereby producing widely variable net quantities of UFP+FPs and CO.⁸⁷ Though it is well known that combustion-generated gases and particles cannot accurately serve as interchangeable indicators of each other in real environments, this evaluation method is valuable to characterize emission conditions, especially when exploring understudied indoor environments. All measurements were passive and without interference of stove use patterns throughout this field campaign; however, it would be interesting to note different stove operational conditions and compare them with PN-CO and PSA-CO correlation regimes in future studies.

4 | CONCLUSIONS

It is important to be able to hold the most polluted environments to the same standards as indoor environments with exemplary factors of indoor environmental quality, which are more easily compared when using the same metrics. Field studies characterizing the contribution of daily activities to indoor air pollution often measure and model UFP+FP concentrations in order to encompass source and loss processes of smaller aerosols generated from events such as cleaning, cooking, electric appliance usage, and outdoor air intake.^{27,29,109-111} Thus, field campaigns such as this which investigate the effects of architectural design and stove variations in mitigating indoor woodsmoke aerosol concentrations must carefully consider metrics of success. Though the common ways of deciding original and improved stove tiers based on mass metrics, such as PM_1 , $PM_{2.5}$, elemental carbon, and brown carbon, are highly systematic and widely effective for comparing cooking environments with the same stove types,²⁵ it is clear that cookstoves with improved combustion such as rocket, gasifier, and air injection have the potential to release a greater abundance of particles smaller than 30nm relative to TSFs (exemplified in

Figure 1).^{49,112} Thus, number- and surface area-based metrics are imperative when comparing effects due to different combustion sources, such as improved cookstoves.

This study demonstrates that field-portable diffusion chargers are a reliable aerosol measurement technique for capturing emissions and exposures of ultrafine and fine woodsmoke aerosol ($D_p \sim 10\text{--}2500\text{ nm}$) in wood-burning kitchens. Field deployment of calibrated diffusion chargers across nine kitchens in Nandi County, Kenya revealed that PN and PSA concentrations of UFP+FPs vary considerably during the day due to frequent cooking activities, are influenced by kitchen design and ventilation features, and cannot be accurately predicted using CO concentrations. The lowest PN and PSA concentrations were observed in a kitchen that included a variety of natural ventilation features that enhanced indoor-to-outdoor transport of UFP+FPs. The range in indoor PN (10^3 to $>10^6/\text{cm}^3$) and PSA ($10^2\text{--}10^5\text{ }\mu\text{m}^2/\text{cm}^3$) concentrations can inform the suitability of field sampling strategies for monitoring woodsmoke aerosol size distributions via electrical mobility and aerodynamic size classification techniques. PN and PSA size distributions can be coupled with deposition fractions for the human respiratory tract to estimate inhaled deposited dose rates.^{113–116}

The field measurements in the Nandi kitchens can guide the development and application of low-cost aerosol sensing technologies for deployment in biomass burning environments. There has been significant research on the design, assessment, and use of low-cost optical particle counters, however, such sensors cannot reliably detect sub-300nm particles.^{52–54} Thus, efforts are needed to develop low-cost, battery-powered diffusion chargers and CPCs for long-term monitoring of sub-300nm woodsmoke aerosol in rural communities in sub-Saharan Africa, Asia, and Central America, where UFP+FP data is limited. This will allow for more accurate estimates of exposure-dose-response relationships of inhaled UFP+FPs in field environments and more effectively tailored mitigation strategies. Concurrent monitoring of PN and PSA concentrations and size distributions, CO concentrations, and carbon dioxide (CO_2) concentrations can also improve evaluation of stove combustion conditions in field settings. Coupling these measurements in future studies alongside traditional mass-based measurements will allow for comparisons across existing studies in similar rural environments, while capturing smaller aerosol size fractions to present a more comprehensive view of biomass combustion emissions^{24,46} and contributing to a larger body of knowledge of UFP+FPs in lesser studied environments.

AUTHOR CONTRIBUTIONS

DNW conducted the field measurements in the Nandi kitchens, with support from SRO and under the guidance of RMA and BEB. DNW analyzed the ultrafine and fine woodsmoke aerosol and carbon monoxide concentration data. DNW wrote the manuscript, with input from all coauthors.

ACKNOWLEDGMENTS

The authors are thankful for the help and support of Irene Kalamai (AMPATH Kenya), Dr. Joseph J. Mamlin (Indiana University School of Medicine and AMPATH Kenya), Dr. David K. Lagat (Moi University

School of Medicine), Nathan Vazquez (Purdue University), Qianrui Gao (Purdue University), Oliver S. Schroeder (Purdue University), and Michael Tishchenko (Purdue University).

FUNDING INFORMATION

Financial support was provided by the National Science Foundation (CBET-1847493 to BEB), the Purdue University Shah Family Global Innovation Lab (to DNW, SRO, RMA, and BEB), and an American Society of Heating, Refrigerating, and Air Conditioning Engineers Graduate Student Grant-In-Aid Award (to DNW).

CONFLICT OF INTEREST

The authors declare no competing financial interest.

DATA AVAILABILITY STATEMENT

The data that support the findings of this study are available from the corresponding author upon reasonable request.

ETHICS APPROVAL STATEMENT

The Purdue University Human Research Protection Program reviewed the research project (IRB-2019-885) and determined that the project qualifies as exempt from Institutional Review Board review.

ORCID

Danielle N. Wagner  <https://orcid.org/0000-0001-6572-9001>

Rose M. Ayikukwei  <https://orcid.org/0000-0002-6429-1332>

Brandon E. Boor  <https://orcid.org/0000-0003-1011-4100>

REFERENCES

- Smith K. Indoor air pollution in developing countries: recommendations for research. *Indoor Air*. 2002;12(5):198–207. doi:10.1016/s0140-6701(03)92121-7
- Evangelopoulos D, Perez-Velasco R, Walton H, et al. The role of burden of disease assessment in tracking progress towards achieving WHO global air quality guidelines. *Int J Public Health*. 2020;65(8):1455–1465. doi:10.1007/s00038-020-01479-z
- Forouzanfar MH, Afshin A, Alexander LT, et al. Global, regional, and national comparative risk assessment of 79 behavioural, environmental and occupational, and metabolic risks or clusters of risks, 1990–2015: a systematic analysis for the Global Burden of Disease Study 2015. *Lancet*. 2016;388(10053):1659–1724. doi:10.1016/S0140-6736(16)31679-8
- World Health Organization. Indoor Air Quality Guidelines: Household Fuel Combustion. World Health Organization. 2014:1–172. http://apps.who.int/iris/bitstream/10665/141496/1/9789241548885_eng.pdf?ua=1
- Gordon SB, Bruce NG, Grigg J, et al. Respiratory risks from household air pollution in low and middle income countries. *Lancet Respir Med*. 2014;2(10):823–860. doi:10.1016/S2213-2600(14)70168-7
- International Energy Agency. World Energy Outlook. 2006. <https://www.iea.org/reports/world-energy-outlook-2006>
- International Energy Agency. Energy Access Outlook 2017. *World Energy Outlook Special Report*. 2017;4(1):59–70. doi:10.1016/0022-2828(72)90097-1
- Smith KR, Bruce N, Balakrishnan K, et al. Millions dead: how do we know and what does it mean? Methods used in

- the comparative risk assessment of household air pollution. *Annu Rev Public Health*. 2014;35(1):185-206. doi:10.1146/annurev-publhealth-032013-182356
9. Wathore R, Mortimer K, Grieshop AP. In-use emissions and estimated impacts of traditional, natural- and forced-draft cookstoves in rural Malawi. *Environ Sci Technol*. 2017;51(3):1929-1938. doi:10.1021/acs.est.6b05557
 10. Njenga M, Iiyama M, Jamnadass R, et al. Gasifier as a cleaner cooking system in rural Kenya. *J Clean Prod*. 2016;121:208-217. doi:10.1016/j.jclepro.2016.01.039
 11. Aung TW, Jain G, Sethuraman K, et al. Health and climate-relevant pollutant concentrations from a carbon-finance approved cookstove intervention in rural India. *Environ Sci Technol*. 2016;50(13):7228-7238. doi:10.1021/acs.est.5b06208
 12. Kar A, Rehman IH, Burney J, et al. Real-time assessment of black carbon pollution in Indian households due to traditional and improved biomass cookstoves. *Environ Sci Technol*. 2012;46(17):9811. doi:10.1021/es303338u
 13. Kituyi E, Marufu L, Wandiga SO, Jumba IO, Andreae MO, Helas G. Carbon monoxide and nitric oxide from biofuel fires in Kenya. *Energy Convers Manag*. 2001;42(13):1517-1542. doi:10.1016/S0196-8904(00)00158-8
 14. Debnath R, Bardhan R, Banerjee R. Investigating the age of air in rural Indian kitchens for sustainable built-environment design. *J Build Eng*. 2016;7:320-333. doi:10.1016/j.jobbe.2016.07.011
 15. Roden CA, Bond TC, Conway S, Osoto Pinel AB, MacCarty N, Still D. Laboratory and field investigations of particulate and carbon monoxide emissions from traditional and improved cookstoves. *Atmos Environ*. 2009;43(6):1170-1181. doi:10.1016/j.atmosenv.2008.05.041
 16. Heinzel AP, Guarnieri MJ, Mann JK, et al. Lung function in woodsmoke-exposed Guatemalan children following a chimney stove intervention. *Thorax*. 2016;71(5):421-428. doi:10.1136/thoraxjnl-2015-207783
 17. Kelp MM, Grieshop AP, Reynolds CCO, et al. Real-time indoor measurement of health and climate-relevant air pollution concentrations during a carbon-finance-approved cookstove intervention in rural India. *Dev Eng*. 2018;3:125-132. doi:10.1016/j.deveng.2018.05.001
 18. Begum BA, Paul SK, Dildar Hossain M, Biswas SK, Hopke PK. Indoor air pollution from particulate matter emissions in different households in rural areas of Bangladesh. *Build Environ*. 2009;44(5):898-903. doi:10.1016/j.buildenv.2008.06.005
 19. de la Sota C, Lumbreras J, Pérez N, et al. Indoor air pollution from biomass cookstoves in rural Senegal. *Energy Sustain Dev*. 2018;43:224-234. doi:10.1016/j.esd.2018.02.002
 20. Douglas Goetz J, Giordano MR, Stockwell CE, et al. Speciated online PM1 from South Asian combustion sources-Part 1: fuel-based emission factors and size distributions. *Atmos Chem Phys*. 2018;18(19):14653-14679. doi:10.5194/acp-18-14653-2018
 21. Siddiqui AR, Lee K, Bennett D, et al. Indoor carbon monoxide and PM2.5 concentrations by cooking fuels in Pakistan. *Indoor Air*. 2009;19(1):75-82. doi:10.1111/j.1600-0668.2008.00563.x
 22. Modera MP. Monitoring the heat output of a wood-burning stove. *Heat Transf Eng*. 1986;7(1-2):25-35. doi:10.1080/01457638608939642
 23. Chen Y, Roden CA, Bond TC. Characterizing biofuel combustion with patterns of real-time emission data (PaRTED). *Environ Sci Technol*. 2012;46(11):6110-6117. doi:10.1021/es3003348
 24. Zhang H, Wang S, Hao J, et al. Chemical and size characterization of particles emitted from the burning of coal and wood in rural households in Guizhou, China. *Atmos Environ*. 2012;51:94-99. doi:10.1016/j.atmosenv.2012.01.042
 25. Armendáriz-Arnez C, Edwards RD, Johnson M, Rosas IA, Espinosa F, Masera OR. Indoor particle size distributions in homes with open fires and improved Patsari cook stoves. *Atmos Environ*. 2010;44(24):2881-2886. doi:10.1016/j.atmosenv.2010.04.049
 26. Hussein T, Hämeri K, Heikkinen MSA, Kulmala M. Indoor and outdoor particle size characterization at a family house in Espoo-Finland. *Atmos Environ*. 2005;39(20):3697-3709. doi:10.1016/j.atmosenv.2005.03.011
 27. Patel S, Sankhyani S, Boedicker EK, et al. Indoor particulate matter during HOMEChem: concentrations, size distributions, and exposures. *Environ Sci Technol*. 2020;54(12):7107-7116. doi:10.1021/acs.est.0c00740
 28. Wu T, Boor BE. Urban aerosol size distributions: a global perspective. *Atmos Chem Phys*. 2021;21(11):8883-8914. doi:10.5194/acp-21-8883-2021
 29. Jiang J, Jung N, Boor BE. Using building energy and smart thermostat data to evaluate indoor ultrafine particle source and loss processes in a net-zero energy house. *ACS EST Engg*. 2021;1(4):780-793. doi:10.1021/acsestengg.1c00002
 30. Seinfeld JH, Pandis SN. *Atmospheric chemistry and physics: From air pollution to climate change* (3rd ed.) John Wiley & Sons; 2016. <https://www.wiley.com/en-us/Atmospheric+Chemistry+and+Physics:+From+Air+Pollution+to+Climate+Change,+3rd+Edition-p-9781118947401>
 31. Hussein T, Alameer A, Jaghbeir O, et al. Indoor particle concentrations, size distributions, and exposures in middle eastern microenvironments. *Atmosphere*. 2021;11(1):41. doi:10.3390/atmos12040515
 32. Riley WJ, McKone TE, Lai ACK, Nazaroff WW. Indoor particulate matter of outdoor origin importance of size-dependent removal mechanisms. *Environ Sci Technol*. 2002;36(2):200-207. doi:10.1021/es010723y
 33. Leskinen J, Ihalainen M, Torvela T, et al. Effective density and morphology of particles emitted from small-scale combustion of various wood fuels. *Environ Sci Technol*. 2014;48(22):13298-13306. doi:10.1021/es502214a
 34. Uski O, Jalava PI, Happonen MS, et al. Different toxic mechanisms are activated by emission PM depending on combustion efficiency. *Atmos Environ*. 2014;89:623-632. doi:10.1016/j.atmosenv.2014.02.036
 35. Jalava PI, Salonen RO, Nuutinen K, et al. Effect of combustion condition on cytotoxic and inflammatory activity of residential wood combustion particles. *Atmos Environ*. 2010;44(13):1691-1698. doi:10.1016/j.atmosenv.2009.12.034
 36. Schmid O, Stoeger T. Surface area is the biologically most effective dose metric for acute nanoparticle toxicity in the lung. *J Aerosol Sci*. 2016;99:133-143. doi:10.1016/j.jaerosci.2015.12.006
 37. Arora P, Jain S. Morphological characteristics of particles emitted from combustion of different fuels in improved and traditional cookstoves. *J Aerosol Sci*. 2015;82:13-23. doi:10.1016/j.jaerosci.2014.12.006
 38. Arora P, Jain S, Sachdeva K. Physical characterization of particulate matter emitted from wood combustion in improved and traditional cookstoves. *Energy Sustain Dev*. 2013;17(5):497-503. doi:10.1016/j.esd.2013.06.003
 39. Corsini E, Ozgen S, Papale A, et al. Insights on wood combustion generated proinflammatory ultrafine particles (UFP). *Toxicol Lett*. 2017;266:74-84. doi:10.1016/j.toxlet.2016.12.005
 40. Stoeger T, Takenaka S, Frankenberger B, et al. Deducing in vivo toxicity of combustion-derived nanoparticles from a cell-free oxidative potency assay and metabolic activation of organic compounds. *Environ Health Perspect*. 2009;117(1):54-60. doi:10.1289/ehp.11370
 41. Oberdörster G, Oberdörster E, Oberdörster J. Nanotoxicology: an emerging discipline evolving from studies of ultrafine particles. *Environ Health Perspect*. 2005;113(7):823-839. doi:10.1289/ehp.7339

42. Naeher LP, Brauer M, Lipsett M, et al. Woodsmoke health effects: a review. *Inhal Toxicol*. 2007;19(1):67-106. doi:10.1080/08958370600985875
43. Weggler BA, Ly-Verdu S, Jennerwein M, et al. Untargeted identification of wood type-specific markers in particulate matter from wood combustion. *Environ Sci Technol*. 2016;50(18):10073-10081. doi:10.1021/acs.est.6b01571
44. Li N, He F, Liao B, Zhou Y, Li B, Ran P. Exposure to ambient particulate matter alters the microbial composition and induces immune changes in rat lung. *Respir Res*. 2017;18(1):1-10. doi:10.1186/s12931-017-0626-6
45. Tyler CR, Zychowski KE, Sanchez BN, et al. Surface area-dependence of gas-particle interactions influences pulmonary and neuroinflammatory outcomes. *Part Fibre Toxicol*. 2016;13(1):1-18. doi:10.1186/s12989-016-0177-x
46. Leavey A, Londeree J, Priyadarshini P, et al. Real-time particulate and CO concentrations from cookstoves in rural households in Udaipur, India. *Environ Sci Technol*. 2015;49(12):7423-7431. doi:10.1021/acs.est.5b02139
47. Rapp VH, Caubel JJ, Wilson DL, Gadgil AJ. Reducing ultrafine particle emissions using air injection in wood-burning cookstoves. *Environ Sci Technol*. 2016;50(15):8368-8374. doi:10.1021/acs.est.6b01333
48. Jetter J, Zhao Y, Smith KR, et al. Pollutant emissions and energy efficiency under controlled conditions for household biomass cookstoves and implications for metrics useful in setting international test standards. *Environ Sci Technol*. 2012;46(19):10827-10834. doi:10.1021/es301693f
49. Just B, Rogak S, Kandlikar M. Characterization of ultrafine particulate matter from traditional and improved biomass cookstoves. *Environ Sci Technol*. 2013;47(7):3506-3512. doi:10.1021/es304351p
50. Cassee FR, Héroux ME, Gerlofs-Nijland ME, Kelly FJ. Particulate matter beyond mass: recent health evidence on the role of fractions, chemical constituents and sources of emission. *Inhal Toxicol*. 2013;25(14):802-812. doi:10.3109/08958378.2013.850127
51. World Health Organization. Air quality guidelines for particulate matter, ozone, nitrogen dioxide and sulfur dioxide: Global update 2005. Published online 2005:1-21. doi:10.1016/0004-6981(88)90109-6
52. Patra SS, Ramsisaria R, Du R, Wu T, Boor BE. A machine learning field calibration method for improving the performance of low-cost particle sensors. *Build Environ*. 2021;190:107457. doi:10.1016/j.buildenv.2020.107457
53. Hagan D, Kroll J. Assessing the accuracy of low-cost optical particle sensors using a physics-based approach. *Atmos Meas Tech*. 2020;13(11):6343-6355. doi:10.5194/amt-2020-188
54. Giordano MR, Malings C, Pandis SN, et al. From low-cost sensors to high-quality data: a summary of challenges and best practices for effectively calibrating low-cost particulate matter mass sensors. *J Aerosol Sci*. 2021;158:105833. doi:10.1016/j.jaerosci.2021.105833
55. Sahu M, Peipert J, Singhal V, Yadama GN, Biswas P. Evaluation of mass and surface area concentration of particle emissions and development of emissions indices for cookstoves in rural India. *Environ Sci Technol*. 2011;45(6):2428-2434. doi:10.1021/es1029415
56. Wangchuk T, He C, Knibbs LD, Mazaheri M, Morawska L. A pilot study of traditional indoor biomass cooking and heating in rural Bhutan: gas and particle concentrations and emission rates. *Indoor Air*. 2017;27(1):160-168. doi:10.1111/ina.12291
57. Maricq MM. Monitoring Motor vehicle PM emissions: an evaluation of three portable low-cost aerosol instruments. *Aerosol Sci Tech*. 2013;47(5):564-573. doi:10.1080/02786826.2013.773394
58. Hyun J, Han J, Lee SG, Hwang J. Design and performance evaluation of a PN1 sensor for real-time measurement of indoor aerosol size distribution. *Aerosol Air Qual Res*. 2018;18(2):285-300. doi:10.4209/aaqr.2017.08.0263
59. Kim HL, Han J, Lee SM, Kwon HB, Hwang J, Kim YJ. MEMS-based particle detection system for measuring airborne ultrafine particles. *Sens Actuators A Phys*. 2018;283:235-244. doi:10.1016/j.sna.2018.09.060
60. Canha N, Lage J, Coutinho JT, Alves C, Almeida SM. Comparison of indoor air quality during sleep in smokers and non-smokers' bedrooms: a preliminary study. *Environ Pollut*. 2019;249:248-256. doi:10.1016/j.envpol.2019.03.021
61. Kenya National Bureau of Statistics. County statistical. 2015:1-75. https://www.knbs.or.ke/?page_id=3142&wpdmc=county-statistical-abstracts
62. Kenya National Bureau of Statistics. Kenya Population and Housing Census 2009, Household source of cooking fuel by county and district. 2008:1-8.
63. Lagat DK, Delong AK, Wellenius GA, et al. Factors associated with isolated right heart failure in women a pilot study from western Kenya. *Glob Heart*. 2014;9(2):249-254. doi:10.1016/j.ghheart.2014.04.003
64. Bloomfield GS, Lagat DK, Akwanalo OC, et al. Conditions that predispose to pulmonary hypertension and right heart failure in persons exposed to household air pollution in LMIC. *Glob Heart*. 2012;7(3):249-259. doi:10.1016/j.ghheart.2012.06.015
65. Diette GB, Accinelli RA, Balmes JR, et al. Obstructive lung disease and exposure to burning biomass fuel in the indoor environment. *Glob Heart*. 2012;7(3):265-270. doi:10.1016/j.ghheart.2012.06.016
66. Rudin P, Gordon D, Maginot C, Webb E. Clear as mud: analyzing soil composition. *J Purdue Undergrad Res*. 2018;8(1):24. doi:10.5703/1288284316745
67. Coorstek Sensors. Pegasor AQ indoor air quality monitor. *Operating Manual*. 2016;(1):42. doi:10.4401/ag-3560
68. Amanatidis S, Maricq MM, Ntziachristos L, Samaras Z. Measuring number, mass, and size of exhaust particles with diffusion chargers: the dual Pegasor particle sensor. *J Aerosol Sci*. 2016;92:1-15. doi:10.1016/j.jaerosci.2015.10.005
69. Rostedt A, Arffman A, Janka K, Yli-Ojanperä J, Keskinen J. Characterization and response model of the PPS-M aerosol sensor. *Aerosol Sci Technol*. 2014;48(10):1022-1030. doi:10.1080/02786826.2014.951023
70. Lanki T, Tikkanen J, Janka K, Taimisto P, Lehtimäki M. An electrical sensor for long-term monitoring of ultrafine particles in workplaces. *J Phys Conf Ser*. 2011;304(1):012013. doi:10.1088/1742-6596/304/1/012013
71. Wu T, Boor BE. Characterization of a thermal aerosol generator for HVAC filtration experiments (RP-1734). *Sci Technol Built Environ*. 2020;26(6):816-834. doi:10.1080/23744731.2020.1730661
72. Mendes L, Kangas A, Kukko K, et al. Characterization of emissions from a desktop 3D printer. *J Ind Ecol*. 2017;21:S94-S106. doi:10.1111/jiec.12569
73. Sociaal-Economische Raad. Provisional nano reference values for engineered nanomaterials. Advisory Report 12/01. 2012. ISBN: 978-94-6134-035-1.
74. Saha PK, Hankey S, Marshall JD, Robinson AL, Presto AA. High-spatial-resolution estimates of ultrafine particle concentrations across the continental United States. *Environ Sci Technol*. 2021;55(15):10320-10331. doi:10.1021/acs.est.1c03237
75. Kumar P, Morawska L, Birmili W, et al. Ultrafine particles in cities. *Environ Int*. 2014;66:1-10. doi:10.1016/j.envint.2014.01.013
76. Gani S, Chambliss SE, Messier KP, Lunden MM, Apte JS. Spatiotemporal profiles of ultrafine particles differ from other traffic-related air pollutants: lessons from long-term

- measurements at fixed sites and mobile monitoring. *Environ Sci Atmos*. 2021;1(7):558-568. doi:10.1039/d1ea00058f
77. Apte JS, Kirchstetter TW, Reich AH, et al. Concentrations of fine, ultrafine, and black carbon particles in auto-rickshaws in New Delhi, India. *Atmos Environ*. 2011;45(26):4470-4480. doi:10.1016/j.atmosenv.2011.05.028
 78. Wan MP, Wu CL, Sze To GN, Chan TC, Chao CYH. Ultrafine particles, and PM_{2.5} generated from cooking in homes. *Atmos Environ*. 2011;45(34):6141-6148. doi:10.1016/j.atmosenv.2011.08.036
 79. Zhang Q, Gangupomu RH, Ramirez D, Zhu Y. Measurement of ultrafine particles and other air pollutants emitted by cooking activities. *Int J Environ Res Public Health*. 2010;7(4):1744-1759. doi:10.3390/ijerph7041744
 80. Virudachalam S, Long JA, Harhay MO, Polsky DE, Feudtner C. Prevalence and patterns of cooking dinner at home in the USA: National Health and Nutrition Examination Survey (NHANES) 2007-2008. *Public Health Nutr*. 2014;17(5):1022-1030. doi:10.1017/S1368980013002589
 81. Bhangar S, Mullen NA, Hering SV, Kreisberg NM, Nazaroff WW. Ultrafine particle concentrations and exposures in seven residences in Northern California. *Indoor Air*. 2011;21(2):132-144. doi:10.1111/j.1600-0668.2010.00689.x
 82. Rhodes EL, Dreifelbis R, Klasen E, et al. Behavioral attitudes and preferences in cooking practices with traditional open-fire stoves in Peru, Nepal, and Kenya: implications for improved cookstove interventions. *Int J Environ Res Public Health*. 2014;11(10):10310-10326. doi:10.3390/ijerph111010310
 83. Benka-Coker ML, Peel JL, Volckens J, et al. Kitchen concentrations of fine particulate matter and particle number concentration in households using biomass cookstoves in rural Honduras. *Environ Pollut*. 2020;258:113697. doi:10.1016/j.envpol.2019.113697
 84. Chowdhury Z, Le LT, Masud A, et al. Quantification of indoor air pollution from using cookstoves and estimation of its health effects on adult women in Northwest Bangladesh. *Aerosol Air Qual Res*. 2012;12(4):463-475. doi:10.4209/aaqr.2011.10.0161
 85. Ntziachristos L, Polidori A, Phuleria H, Geller MD, Sioutas C. Application of a diffusion charger for the measurement of particle surface concentration in different environments. *Aerosol Sci Tech*. 2007;41(6):571-580. doi:10.1080/02786820701272020
 86. Mullen NA, Liu C, Zhang Y, Wang S, Nazaroff WW. Ultrafine particle concentrations and exposures in four high-rise Beijing apartments. *Atmos Environ*. 2011;45(40):7574-7582. doi:10.1016/j.atmosenv.2010.07.060
 87. Kocbach Bølling A, Pagels J, Yttri KE, et al. Health effects of residential wood smoke particles: the importance of combustion conditions and physicochemical particle properties. *Part Fibre Toxicol*. 2009;6(1):1-20. doi:10.1186/1743-8977-6-29
 88. Shen G, Gaddam CK, Ebersviller SM, et al. A laboratory comparison of emission factors, number size distributions, and morphology of ultrafine particles from 11 different household cookstove-fuel systems. *Environ Sci Technol*. 2017;51(11):6522-6532. doi:10.1021/acs.est.6b05928
 89. Hussein T, Glytsos T, Ondráček J, et al. Particle size characterization and emission rates during indoor activities in a house. *Atmos Environ*. 2006;40(23):4285-4307. doi:10.1016/j.atmosenv.2006.03.053
 90. Glytsos T, Ondráček J, Džumbová L, Kopanakis I, Lazaridis M. Characterization of particulate matter concentrations during controlled indoor activities. *Atmos Environ*. 2010;44(12):1539-1549. doi:10.1016/j.atmosenv.2010.01.009
 91. Hussein T, Korhonen H, Herrmann E, Hämeri K, Lehtinen KEJ, Kulmala M. Emission rates due to indoor activities: indoor aerosol model development, evaluation, and applications. *Aerosol Sci Tech*. 2005;39(11):1111-1127. doi:10.1080/02786820500421513
 92. Ezzati M, Mbinda BM, Kammen DM. Comparison of emissions and residential exposure from traditional and improved cookstoves in Kenya. *Environ Sci Technol*. 2000;34(4):578-583. doi:10.1021/es9905795
 93. Morawska L, Ristovski Z, Jayaratne ER, Keogh DU, Ling X. Ambient nano and ultrafine particles from motor vehicle emissions: characteristics, ambient processing and implications on human exposure. *Atmos Environ*. 2008;42(35):8113-8138. doi:10.1016/j.atmosenv.2008.07.050
 94. Ngo NS, Gatari M, Yan B, Chillrud SN, Bouhamam K, Kinney PL. Occupational exposure to roadway emissions and inside informal settlements in sub-Saharan Africa: a pilot study in Nairobi, Kenya. *Atmos Environ*. 2015;111:179-184. doi:10.1016/j.atmosenv.2015.04.008
 95. Andreae MO. Ozone and Aitken nuclei over equatorial Africa: airborne observations during DECAFE 88. *J Geophys Res*. 1992;97(D6):6137-6148. doi:10.1029/91JD00961
 96. Pósfai M, Simonic R, Li J, Hobbs PV, Buseck PR. Individual aerosol particles from biomass burning in southern Africa: 1. Compositions and size distributions of carbonaceous particles. *J Geophys Res Atmos*. 2003;108(13):1-13. doi:10.1029/2002jd002291
 97. Heintzenberg J, Hermann M, Theiss D. Out of Africa: high aerosol concentrations in the upper troposphere over Africa. *Atmos Chem Phys*. 2003;3(4):1191-1198. doi:10.5194/acp-3-1191-2003
 98. Hirsikko A, Vakkari V, Tiitta P, et al. Characterisation of sub-micron particle number concentrations and formation events in the western Bushveld Igneous Complex, South Africa. *Atmos Chem Phys*. 2012;12(9):3951-3967. doi:10.5194/acp-12-3951-2012
 99. Sunnu A, Afeti G, Resch F. A long-term experimental study of the Saharan dust presence in West Africa. *Atmos Res*. 2008;87(1):13-26. doi:10.1016/j.atmosres.2007.07.004
 100. Pacitto A, Stabile L, Morawska L, et al. Daily submicron particle doses received by populations living in different low- and middle-income countries. *Environ Pollut*. 2021;269:116229. doi:10.1016/j.envpol.2020.116229
 101. Zhang S, Broday DM, Raz R. Predictors of the indoor-to-outdoor ratio of particle number concentrations in Israel. *Atmosphere*. 2020;11(10):1074. doi:10.3390/atmos11101074
 102. Matson U. Indoor and outdoor concentrations of ultrafine particles in some Scandinavian rural and urban areas. *Sci Total Environ*. 2005;343(1-3):169-176. doi:10.1016/j.scitotenv.2004.10.002
 103. Klasen EM, Wills B, Naithani N, et al. Low correlation between household carbon monoxide and particulate matter concentrations from biomass-related pollution in three resource-poor settings. *Environ Res*. 2015;142:424-431. doi:10.1016/j.envres.2015.07.012
 104. Clark ML, Bachand AM, Heiderscheidt JM, et al. Impact of a cleaner-burning cookstove intervention on blood pressure in Nicaraguan women. *Indoor Air*. 2013;23(2):105-114. doi:10.1111/ina.12003
 105. Ochieng C, Vardoulakis S, Tonne C. Household air pollution following replacement of traditional open fire with an improved rocket type cookstove. *Sci Total Environ*. 2017;580:440-447. doi:10.1016/j.scitotenv.2016.10.233
 106. Carter E, Norris C, Dionisio KL, et al. Assessing exposure to household air pollution: a systematic review and pooled analysis of carbon monoxide as a surrogate measure of particulate matter. *Environ Health Perspect*. 2017;125(7):1-12. doi:10.1289/EHP767
 107. Patel S, Leavey A, He S, Fang J, O'Malley K, Biswas P. Characterization of gaseous and particulate pollutants from gasification-based improved cookstoves. *Energy Sustain Dev*. 2016;32:130-139. doi:10.1016/j.esd.2016.02.005
 108. Tissari J, Lyrränen J, Hytönen K, et al. Fine particle and gaseous emissions from normal and smouldering wood combustion in a conventional masonry heater. *Atmos Environ*. 2008;42(34):7862-7873. doi:10.1016/j.atmosenv.2008.07.019
 109. Schripp T, Kirsch I, Salthammer T. Characterization of particle emission from household electrical appliances. *Sci Total Environ*. 2011;409(13):2534-2540. doi:10.1016/j.scitotenv.2011.03.033

110. Shehab M, Pope FD, Delgado-Saborit JM. The contribution of cooking appliances and residential traffic proximity to aerosol personal exposure. *J Environ Health Sci Eng*. 2021;19(1):307-318. doi:10.1007/s40201-020-00604-7
111. Chen C, Zhao Y, Zhao B. Emission rates of multiple air pollutants generated from chinese residential cooking. *Environ Sci Technol*. 2018;52(3):1081-1087. doi:10.1021/acs.est.7b05600
112. Caubel JJ, Rapp VH, Chen SS, Gadgil AJ. Optimization of secondary air injection in a wood-burning cookstove: an experimental study. *Environ Sci Technol*. 2018;52(7):4449-4456. doi:10.1021/acs.est.7b05277
113. Jiang J, Ding X, Tasoglou A, et al. Real-time measurements of botanical disinfectant emissions, transformations, and multi-phase inhalation exposures in buildings. *Environ Sci Technol Lett*. 2021;8(7):558-566. doi:10.1021/acs.estlett.1c00390
114. Hussein T, Boor BE, Löndahl J. Regional inhaled deposited dose of indoor combustion-generated aerosols in Jordanian urban homes. *Atmosphere*. 2020;11(11):1150. doi:10.3390/atmos11111150
115. Hussein T, Löndahl J, Paasonen P, et al. Modeling regional deposited dose of submicron aerosol particles. *Sci Total Environ*. 2013;458-460:140-149. doi:10.1016/j.scitotenv.2013.04.022
116. Jiang J, Ding X, Isaacson KP, et al. Ethanol-based disinfectant sprays drive rapid changes in the chemical composition of indoor air in residential buildings. *J Hazard Mater*. 2021;2:100042. doi:10.1016/j.hazl.2021.100042
117. Tryner J, Volckens J, Marchese AJ. Effects of operational mode on particle size and number emissions from a biomass gasifier cookstove. *Aerosol Sci Tech*. 2018;52(1):87-97. doi:10.1080/02786826.2017.1380779
118. Tiwari M, Sahu SK, Bhangare RC, Yousaf A, Pandit GG. Particle size distributions of ultrafine combustion aerosols generated from household fuels. *Atmos Pollut Res*. 2014;5(1):145-150. doi:10.5094/APR.2014.018
119. Human Respiratory Tract Model for Radiological Protection - ICRP 66. *Ann ICRP*. 1994;24:492.

SUPPORTING INFORMATION

Additional supporting information can be found online in the Supporting Information section at the end of this article.

How to cite this article: Wagner DN, Odhiambo SR, Ayikukwei RM, Boor BE. High time-resolution measurements of ultrafine and fine woodsmoke aerosol number and surface area concentrations in biomass burning kitchens: A case study in Western Kenya. *Indoor Air*. 2022;32:e13132. doi: [10.1111/ina.13132](https://doi.org/10.1111/ina.13132)